NANOCLAY REINFORCEMENT EFFECTS ON THERMOMECHANICAL PROPERTIES OF E GLASS/NANOCLAY- EPOXY LAMINATES

A
Thesis Report

Submitted in partial fulfilment of the requirement for the award of degree

MASTER OF ENGINEERING
in
CAD/CAM & ROBOTICS

Submitted By
Rajan Verma
(Roll No. 801081022)

Under Guidance of

Mr. BIKRAMJIT SHARMA
Assistant Professor
Deptt. Of Mechanical Engg.
Thapar University, Patiala

Dr. RAJEEV MEHTA
H.O.D & Associate Professor
Deptt. Of Chemical Engg.
Thapar University, Patiala

MECHANICAL ENGINEERING DEPARTMENT

THAPAR UNIVERSITY, PATIALA-147004, INDIA

July 2012

CERTIFICATE

This is to certify that the work in this thesis report entitled "**Nanoclay Reinforcement Effects On Thermomechanical Properties Of E-Glass/Nanoclay-Epoxy Laminates**" submitted in partial fulfilment of requirement for the award of **Master Of Engineering Degree in CAD/CAM & Robotics** in Mechanical Department of Thapar University, Patiala, is an authentic record of work carried out by me under the guidance of **Mr. Bikramjit Sharma**, Assistant Professor, Mechanical Engineering Department, Thapar University, Patiala and **Dr. Rajeev Mehta**, H.O.D. & Associate Professor, Chemical Engineering Department, Thapar University, Patiala.

The matter embodied in this report has not been submitted in part or full to any university or institute for the award of any degree.

Dated: 15.07.2012

Rajan Verma
Rajan Verma

This is to certify that the above declaration made by the student concern is correct to the best of my knowledge and belief.

Mr. Bikramjit Sharma
Assistant Professor
Deptt. Of Mechanical Engg.
Thapar University, Patiala.

Dr. Rajeev Mehta
H.O.D. & Associate Professor
Deptt. Of Chemical Engg.
Thapar University, Patiala.

Countersigned By:

Dr. Ajay Batish
Professor & H.M.E.D.
Thapar University, Patiala.

Dr. S. K. Mohapatra
Dean Academics Affairs
Thapar University, Patiala.

ACKNOWLEDGEMENT

I am highly grateful to the authorities of Thapar University, Patiala for providing this opportunity to carry out the Thesis work.

I would like to express a deep sense of gratitude and thank profusely my thesis guide **Mr. Bikramjit Sharma**, Assistant Professor, Mechanical Engineering Department, Thapar University, Patiala and **Dr. Rajeev Mehta**, H.O.D. & Associate Professor, Chemical Engineering Department, Thapar University, Patiala for their sincere & invaluable guidance, suggestions and attitude which inspired me to submit report in the present form.

I am highly thankful to **Mr. Toyesh** (Ph.D Scholar in Chemical Engineering Department) for his invaluable guidance & continuous support.

I am also thankful to other faculty members and all the workshop staff of Mechanical Department, Thapar University, Patiala for their support.

I would also like to thank and acknowledge **BASF Construction Chemicals (India) Private Limited and Connell Bros. Mumbai** for supplying us generously with E-Glass Fibre sheet, M Brace epoxy (Base and hardener) and Clay (Closite 30B) etc. for this experimentation.

My special thanks are due to my family members and friends who constantly encouraged me to complete this study.

Rajan Verma

RAJAN VERMA

ABSTRACT

Nanocomposites are a new class of mineral-field plastics that contain relatively small amounts (<10%) of nanometer-sized particles. The particles, due to their extremely high aspect ratios, modulus and high surface area promise to improve structural, mechanical, flame retardant and thermal properties. In the present work, epoxy modified with Closite 30B ® (0.5 wt%, 2 wt%, 3 wt% and 4 wt %) is used with E-glass unidirectional fibers to manufacture three ply laminates having [0^0, 90^0, 0^0] stacking sequence using hand layup method. X ray diffraction of epoxy clay nanocomposites indicate exfoliation of nanoclay at all nanoclay loadings. Tensile test, hardness test and 3-point bending test were performed on fiber reinforced nanocomposites before and after hygrothermal loading. The base line data was generated by performing tests on glass fiber reinforced neat epoxy laminates. The mechanical tests show that the presence of 3 wt% nano-clay largely increases tensile and flexural strength. The micro hardness was found to be maximum at 2 wt% of nanoclay loading. With a further increase in nanoclay loading, a decrease in values of hardness is observed. Further durability studies on nanocomposites have been performed in water and NaOH baths under accelerated hygrothermal conditions. For the 3 wt% specimen the decrease in flexural strength observed after immersion in water and NaOH for 30 days was 57% and 79% respectively. However, the properties degradation in NaOH environment was more severe as compared to simple water.

TABLE OF CONTENT

LIST OF FIGURES

LIST OF TABLES

NOMENCLATURE AND ABBREVATIONS

GFRP	Glass fiber reinforced polymer
VLSI	Very large scale integration
PNC	Polymer nanocomposites
POSS	Polyoctahedral silsesquioxane
OMMT	Monomorillonite organoclay
CNF's	Carbon nanofibers
CNT's	Carbon nanotubes
WXRD	Wide angle x-ray diffraction
ND	Nanodiamond
PAN	Polyacrylonitrile
SEM	Scanning electron microscope
CTE	Coefficient of thermal expansion
VGCF	Vapor grown carbon fiber
CAI	Compression after impact
DSC	Differential scanning calorimetry

CHAPTER 1 INTRODUCTION

Nanotechnology is a very interesting subject which governs the human mind now. From smaller devices like IC's to big buildings nanotechnology has spread its influence. Nanotechnology is the construction and use of functional structures designed from atomic or molecular scale with at least one characteristic dimension measured in nanometers. Their size allows them to exhibit novel and significantly improved physical, chemical, and biological properties, phenomena, and processes because of their size. At nanolevel, some compounds transform from inert to active, from electrical insulator to conductors, from fragile to tough. They can become stronger, lighter and more resistant. These transformed properties are what account for the infinite potential application of nanoparticles. One of the major factors, which alter these properties, is the increase in the ratio of surface area to volume. As the surface area of a particle increases exponentially, creating more sites for bonding, catalysis or reaction with surroundings material, resulting in improved properties such as increased strength or chemical or heat resistance. Hence, due to the high surface-to volume ratio associated with nanometre sized particles it is possible to control the fundamental properties of materials through the surface/size effect. There is a great variety of nanomaterials and their range of properties and possible applications appears to be enormous, from extra-ordinary tiny electronics devices, to biomedical uses and as components of parts of automobiles. In addition to this, in the field of VLSI, nanocomposites can be used as electromagnetic shielding between interconnects. Additionally the fact that nanoparticles have dimensions below the visible wavelength of light, i.e. cannot scatter light, that's why the resulting nanoproduct is transparent, and which has other implications also.

Nanotechnology is directed towards the formation of various nanomaterials such as:

- Nanocomposites
- Nanofiber
- Nanoparticulate fillers

1.1 Nanocomposites

Nanocomposites are new class of materials that describe the combination of two phase materials in which one of the phase dispersed in the matrix has dimension on nanometer scale. Traditional composite materials make use of 10-20% reinforcement material. Nanocomposites can show significant improvement with additions of reinforcement material as small as 1-2%. Nanocomposites are found in nature also, for example in the structure of the abalone shell and bone. The use of nanoparticle-rich materials long predates the understanding of the physical and chemical nature of these materials. The first commercial product of nanoclay-based polymer nano composites was the timing belt cover made from PA6 nanocomposites by Toyota Motors in the early 1990s. Jose-Yacaman *et al.* (1996) investigated the origin of the depth of color and the resistance to acids and bio-corrosion of maya blue paint, attributing it to a nanoparticle mechanism. From the mid 1950s nanoscale organo-clays have been used to control flow of polymer solutions (e.g. as paint viscosifiers) or the constitution of gels (e.g. as a thickening substance in cosmetics, keeping the preparations in homogeneous form).
In mechanical terms, nanocomposites differ from conventional composites due to the exceptionally high surface to volume ratio of the reinforcing phase and/or its exceptionally high aspect ratio. The reinforcing material can be made up of particles (e.g. minerals), sheets (e.g. exfoliated clay stacks) or fibers (e.g. carbon nanotubes). The matrix material properties are significantly affected in the vicinity of the reinforcement.

In order for a material to be considered a nanocomposite, the reinforcement material must have dimensions in the nano-scale. There are particulate composites which have reinforcement material on the micro-scale, these are known as microcomposites. Microcomposites may demonstrate similar properties and improvements to nanocomposites, however nanocomposites are generally more effective with less reinforcement material added to the matrix material.

Advantages of nanocomposites:

• Greater tensile and flexural strength for the same dimension of plastic part
• Reduced weight for the same performance
• Improved mechanical strength
• Improved gas barrier properties for the same film thickness
• Higher chemical resistance

1.2 Polymer nanocomposites

The term "polymer nanocomposite" broadly describes any number of multicomponent systems, where the primary component is the polymer and the filler material has at least one dimension below 100 nm. Polymer nanocomposites are generally lightweight, require low filler loading, are often easy to process and provide property enhancements extending orders of magnitude beyond those realized with traditional composites.

Rapid advancements in nanocomposite technologies have been realized as new classes of nanoscale fillers continue to emerge. Nanoparticles commonly dispersed in polymer matrices include: Polyoctahedral silsesquioxane (POSS), layered silicate clays, carbon nanofibers, carbon nanotubes, and graphite nanoflakes. The structure of these nanoparticles is shown in Figure 1.1. The nano- particles listed above differ in chemistry, morphology, aspect ratio and aggregate size. The nanoparticle chosen for dispersion in a resin is dependent on the intended application. However, realization of significant enhancement in properties with any of the nano-materials requires that the nano-particle is well dispersed throughout the matrix.

Major advantages of the polymer nanocomposites are:

Mechanical properties:

- High adhesion of nanoparticles to polymer matrix result in the enhanced strength of nanocomposites relative to conventional composite.
- Small size of nanoparticles ensures small size of pores in the case of exfoliation of a matrix from filler particles. It results in the strength increase too.
- Introduction of small amount of nanoparticles to polymer significantly enhance the adhesion of polymer to different substance.

Optical properties:

- Nanocomposites are optically more transparent in comparison to conventional composites.
- Special optical effects.
- Optical clarity in comparison to conventionally filled polymers.

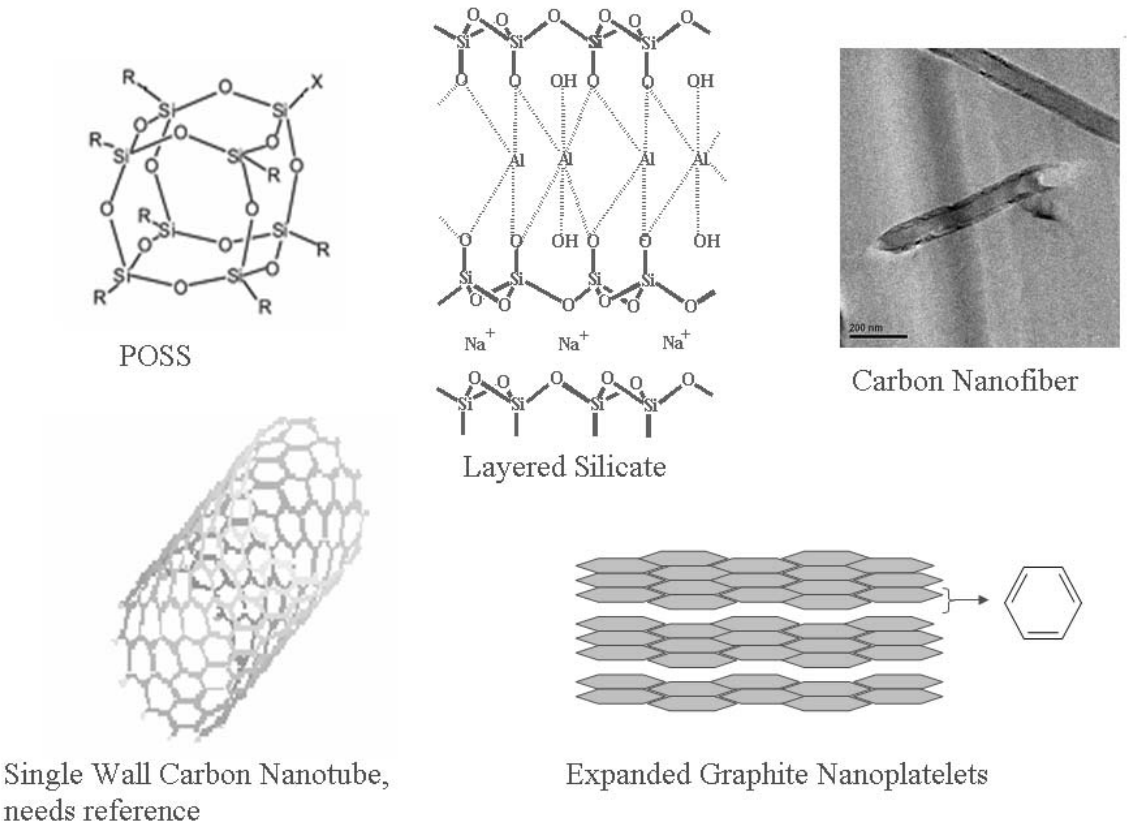

Figure 1.1. Chemical structure or image of commonly investigated nanoparticles[31].

1.3 Epoxy nanocomposites

In 1946, the first industrially-produced epoxy resin was introduced to market. Since then, the use of thermosetting polymers has steadily increased. The wide range of epoxy resin applications includes: coating, electrical, automotive, marine, aerospace and civil infrastructure as well as tool fabrication and pipes and vessels in the chemical industry. Due to their low density of around 1.3 g/cm and good adhesive and mechanical properties, epoxy resin became a promising material for high performance applications in the transport industry, usually in the form of composite materials such as fiber composite or in honeycomb structures. In the aerospace industry, epoxy-composites material can be found in various part of the body and structure of military and civil aircrafts, with the number of applications on the rise. A recent approach to improve and diversify polymer properties in the aerospace industries is through the dispersion of nanometer-scaled

fillers in the polymer matrix. [Njuguna and Pielichowski, 2003]. A significant number of academic and industrial projects have investigated the possibilities to further improve epoxy resin (and in some cases composites or other binary systems) through the strategy of producing nanocomposites.

The term ‘epoxy resin’ refers to both the polymer and its cured resin/hardener system. The former is a low molecular weight oligomer that contains one or more epoxy groups per molecule (more than one unit per molecule is required if the resultant material is to be cross-linked). The characteristic group, a three-member ring known as epoxy, epoxide, oxirane, glycidyl or ethoxyline group is highly strained and therefore very reactive. Epoxy resins can be cross-linked through a polymerization reaction with a hardener at room temperature or at elevated temperature (latent reaction). Curing agents used for room temperature cure are usually aliphatic amines, whilst commonly used higher temperature, higher performance hardener are aromatic amines and acid anhydrides. However, an increasing number of specialized curing agents, such as poly-functional amines, polybasic carboxylic acids, mercaptans and inorganic hardener are also used. All of these results in different, tailored properties of the final polymer matrix. In general, the higher temperature Cured resin systems have improved properties, such as higher glass transition temperatures, strength and stiffness, compared to those cured at room temperature.

1.4 Structure and properties of layered silicates

Silicate consists of small crystalline particles made up of aluminosilicates of various compositions, with possible iron and magnesium substitutions by alkalis and alkaline earth elements. The basic silicon-oxygen unit is a tetrahedron, with four oxygen atoms surrounding the central silicon. The tetrahedra are linked to form hexagonal rings. This pattern repeats in two dimensions to form a sheet. Aluminum, in combination with oxygen, forms an octahedron, with the aluminum at the center, and the octahedral link to form a more closely packed two - dimensional sheet as shown in Figure 1.2.

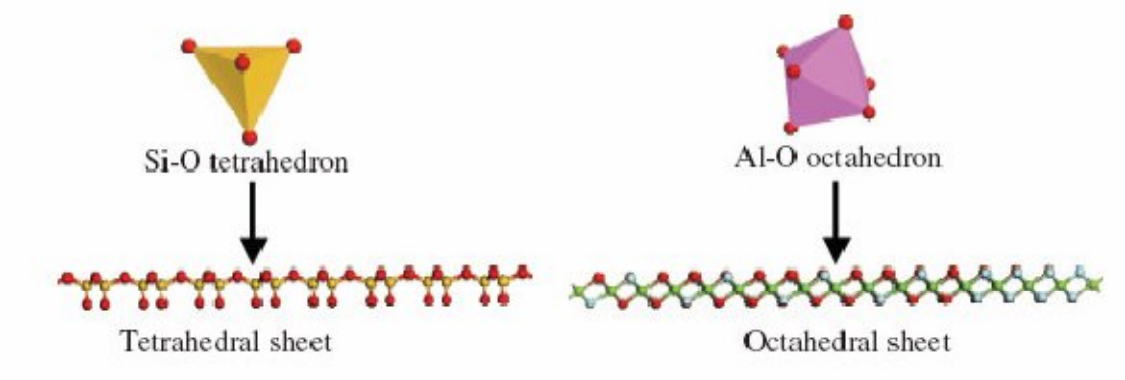

Figure 1.2. Structure of tetrahedral and octahedral sheets[32].

There are two basic types of silicate structures (1: 1 and 2: 1). Kaolinite is an example of 1:1 type of non-swelling dioctahedral silicate. In 2:1 layered silicates two tetrahedral layers surround one octahedral layer, and the oxygen atoms are shared, as an example in montmorillonite.

Silicates used in preparing layered silicate/polymer nanocomposites belong to the 2:1 layered structure type. Montmorillonite (MMT) is one of the most interesting and widely investigated silicates belong to the family of 2:1 layered silicates for polymer nanocomposites because of the weak bonding (Van der Waals) between layers. The chemical formula of MMT silicate is as follows:

$$Na_{0.33}\ (Al_{1.67}Mg_{0.33})\ Si_4O_{10}\ (OH)_2\ nH_2O$$

The crystal structure of montmorillonite consists of two silica tetrahedra fused to an edge shared octahedral sheet of either alumina or magnesia as shown in Figure 1.3. Each layer is composed of a sheet of aluminum or magnesium octahedra sandwiched between two sheets of SiO_4 tetrahedra, which has a unit cell structure consisting of 20 oxygen atoms and 4 OH groups.

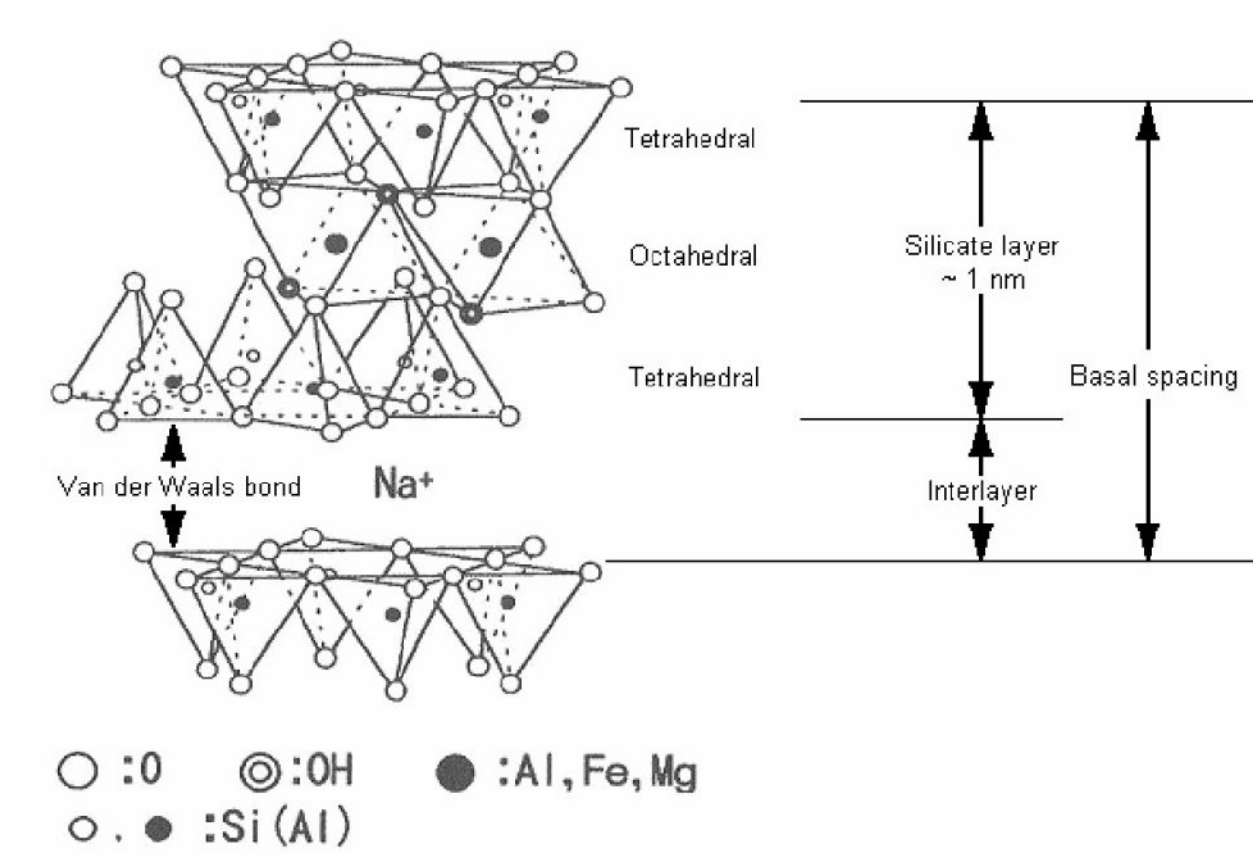

Figure 1.3. Schematic illustration of atomic arrangement in a typical MMT layer[20].

Hundreds or thousands of these layers are stacked together with weak Van der Waals forces to form a silicate particle. Silicate is needed to be organophilic in order to disperse then in monomer phase. So silicate should become organophilic by treatment with suitable modifiers.

1.5 Structure and properties of organically modified layered silicates

Montmorillonite is the most common type of layered silicates used in polymer nanocomposites due to its swellable layered structure. However, the charged nature of the silicate sheets in the silicate makes the silicate sheets incompatible with hydrophobic polymers. The lack of affinity between hydrophilic silicate and hydrophobic polymer tends to agglomeration of the mineral within the polymer matrix. In this case, pre-treatment of the silicate is necessary. Pristine layered silicates (MMT) usually contain hydrated Na^+ or K^+ cations. They can be replaced trough on ion exchange reaction with cationic surfactants, including amino acids, organic ammonium salts, or tetra organic phosphoniums to render the normally hydrophilic silicate surfaces as organophilic. This reaction is illustrated schematically in Figure 1.4. The most popular cationic surfactant is alkylammonium ion because it can be easily exchanged with the ions situated between the silicate layers. Depending on the layer charge density of the silicate, the alkylammonium ions adopt different structures between the silicate layers. The modified silicate becomes organophilic known as organosilicates (OMMT) and it becomes more compatible with organic polymers. The purpose of the pre-treatment is to increase the interlayer spacing as well as to provide better compatibility with polymer.

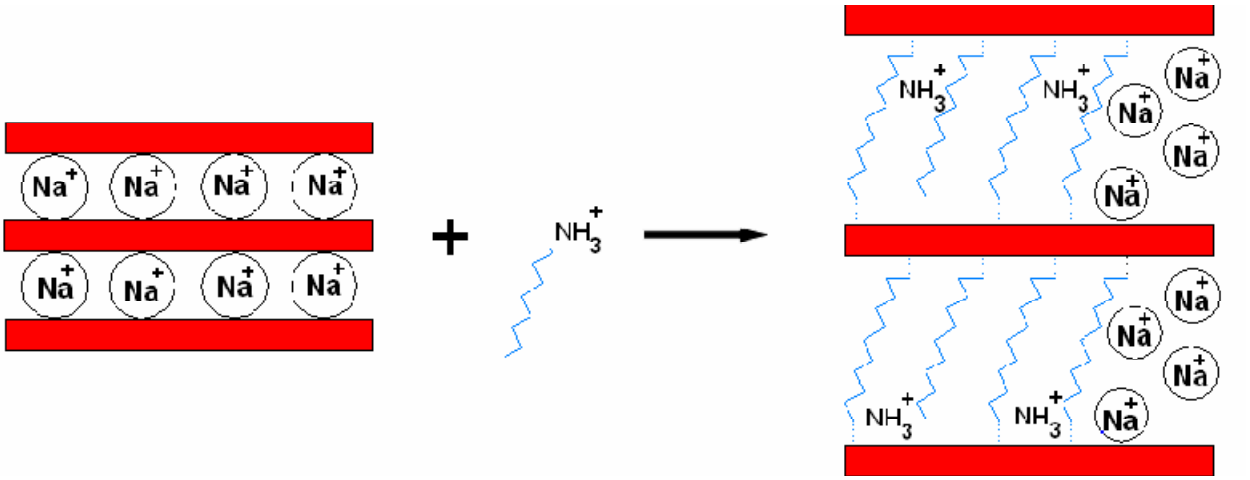

Figure 1.4. Modification of clay surfaces through ion exchange reaction by replacing the Na+ cations with cationic surfactant[32]

1.6 Morphology of nanocomposites

When layered silicates are organically modified and dispersed within a polymer, the spacing expands to allow for the intercalation of polymer between the unit layers.
Depending on the nature of the layered clay and polymer matrix and the level of interactions between them, three different types of polymer nanocomposite morphology are observed. These are: intercalated, exfoliated and phase separated.

1. Phase separated composites: Layered silicates exist in their original aggregated state with no intercalation of the polymer matrix into the galleries (Figure 1.5a). In this case, the particles act as microscale fillers. Their properties stay in the same range as seen in traditional microcomposites.

2. Intercalated composites: When polymer resin is inserted into the gallery between the adjacent layers, the spacing expands, and it is known as the intercalated state (Figure 1.5b). In the intercalated form, matrix polymer molecules are introduced between the ordered layers of silicate resulting in an increase in the interlayer spacing, but still maintaining the order.

3. Exfoliated composites: In an exfoliated nanocomposite, the individual nm scale thick silicate layers are separated and dispersed in a continuous polymer matrix with average distances between layers depending on the silicate concentration (Figure 1.5c). When the layers are fully separated, the silicate is considered to be exfoliated. Exfoliated nanocomposites improve specific properties better than intercalated one, that are affected by the degree of dispersion and resulting interfacial area between polymer and silicate nanolayers.

In addition, partially intercalated or exfoliated composite morphology may also be obtained. In this commonly occurring case, the exfoliated layers and intercalated clusters are randomly distributed in the matrix. The final structure of silicate composite has a wide range of variations, depending on the degree of intercalation and exfoliation. X-ray diffraction measurements are used to characterize the intercalation and exfoliation structures. Reflections in the low angle region indicate intercalated composite, but if the peaks are extremely broad or disappear completely, this indicates complete exfoliation.

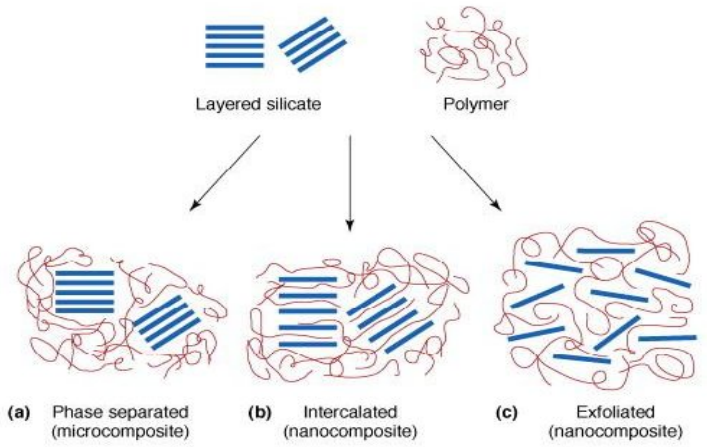

Figure 1.5. Different morphology of layered silicate/polymer nanocomposites[32].

1.7 Glass fiber

Glass fiber is a material made from extremely fine fibers of glass, and it is the largest reinforcement measured in sales. Glass fiber was invented in 1938 by Russell Games Slayter of Owens-Corning as a material to be used as insulation [Lowenstein, 1973]. Ever since then, glass fiber has become widely used as insulation and composite reinforcement material. Based on the composition and the application, glass fibers can be classified in several types.

Figure 1.6. Commercially available glass fibers[15].

The most commonly used glass fiber type for composite applications is E-glass, due to its relatively good mechanical properties and high electrical insulation. S-glass is also used in composite materials where high tensile strength is desired, however this material comes at a much higher cost. R-glass is also used in composite materials with high mechanical requirements such as fatigue life and high chemical resistance. The typical fiber diameter for glass fiber is 9-17 μm and the specific gravity is about 2.5. The tensile strength of glass fiber is in the order of 2000-4800 MPa and the elastic modulus is in the order of 50-90 GPa, much higher than that of polymers [Biron, 1973].

1.8 Carbon fiber

Carbon fiber is another major fiber reinforcement type used in FRPC. One of the most common methods of manufacturing carbon fiber is the oxidation and thermal pyrolysis of polyacrylonitrile (PAN), so called PAN-based carbon fibers. This material consists of extremely thin fibers about 5-10 μm in diameter and comprised mostly of carbon atoms. The carbon atoms are bonded together in microscopic crystals that are mostly aligned parallel to the long axis of the fiber. This alignment makes the fiber show very high tensile properties. The tensile strength of carbon fiber is in the order of 3000-5800 MPa and the elastic modulus is in the order of 500-600 GPa [Lowenstein, 1973].

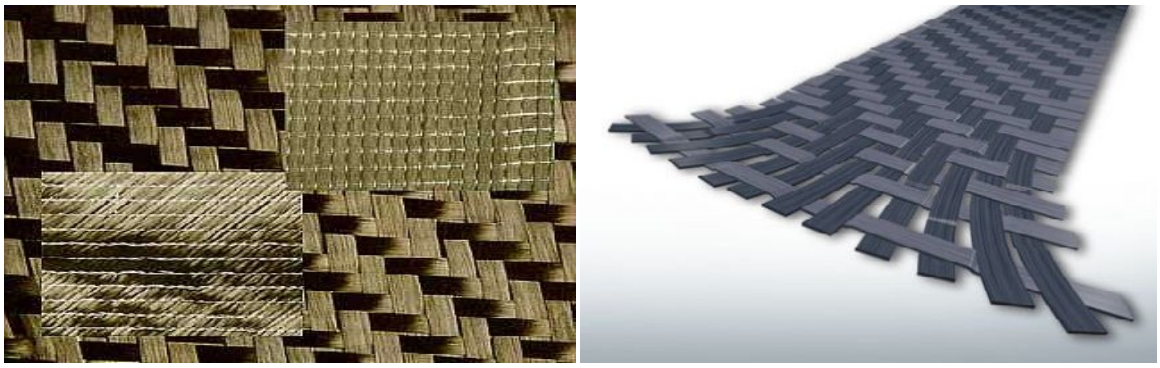

Figure 1.7. Different types of matted carbon fibers[15].

Compared with glass fibers, carbon fibers have lower density but higher tensile strength and elastic modulus. These properties make carbon fiber an ideal reinforcement for composite

materials used in aircraft components, high-performance vehicles, sporting equipment, wind generator blades, and other high demand, high performance applications.

1.8 Environmental effects on fiber composites

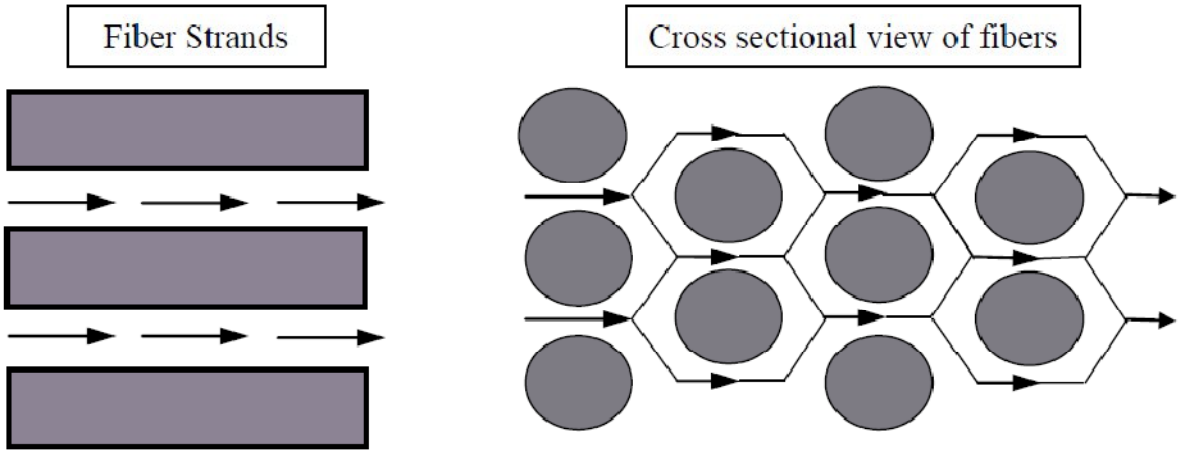

Fig. 1.8 Diffusion path of moisture into composite thickness direction

Fibrous composites, especially carbon fiber reinforced epoxy are increasingly being used in military and aerospace applications owing to several desirable properties including high specific strength, high specific stiffness and controlled anisotropy. Despite these advantages over conventional structural materials such as metals, composites are susceptible to heat and moisture when operating in harsh and changing environmental conditions. When exposed to humid environments, carbon–epoxy composites absorb moisture and undergo dilatational expansion. The presence of moisture and the stresses associated with moisture induced expansion can result in lowered damage tolerance, with an adverse effect on long-term structural durability. The amount of moisture absorbed by the epoxy matrix is significantly greater than that by the carbon fibers, which absorb very little or no moisture. This results in a significant mismatch in the moisture induced volumetric expansion between the matrix and the fibers, and thus leads to the evolution of localized stress and strain fields in the composite.

In homogeneous materials, the kinetics of moisture diffusion is governed by the maximum moisture content and the diffusivity. The maximum moisture content is defined by the net amount of moisture that a fully saturated material contains under steady state equilibrium when exposed to a given environmental condition. It is usually expressed as the ratio of the increase in

weight per unit dry weight at the point of saturation. The relative weight gain approaches the maximum moisture content of composite at infinite time. It has been shown that the maximum moisture content strongly depends on the relative humidity of the exposure environment. Usually the maximum moisture content is determined by exposing the material to a humid environment for a long duration of time until steady state equilibrium is attained. This process often takes several months, which makes the procedure cumbersome and time consuming. Also the rate of moisture diffusion is governed by the diffusivity. In general, the diffusivity is a strong function of the ambient temperature and a weak function of the relative humidity. In the case of composites, the diffusion process is more complex. It depends on the diffusivities of the individual constituents, their relative volume fractions, constituent arrangement and morphology. Traditionally, effective diffusivity has been used to predict the amount of moisture content. The figure 1.7 shows the various effects of moisture diffusion on a composite sample. When a fiber-reinforced composite material is exposed to a hygrothermal environment and mechanical loads, changes in material properties are expected. These changes in material properties are connected to an irreversible material degradation. The moisture may affect the laminates through chemical changes such as relaxation and oxidation of the matrix material. A cyclic moisture environment exposed laminate may experience damage such as debonding at fiber/matrix interfaces and continuous cracks. Usually one of the first observed damage modes in a laminated composite is *matrix cracking*. These cracks are in general not critical for final failure, but if they are connected to a surrounding moisture environment more rapid moisture absorption may be expected for the cracked laminate. The accelerated moisture absorption in a cracked material exposed to humid air is a result of the faster diffusion in air compared to the diffusion speed in the composite material. Faster moisture uptake may also develop a faster material degradation. This makes it important to know the moisture absorption behaviour in a cracked laminate.

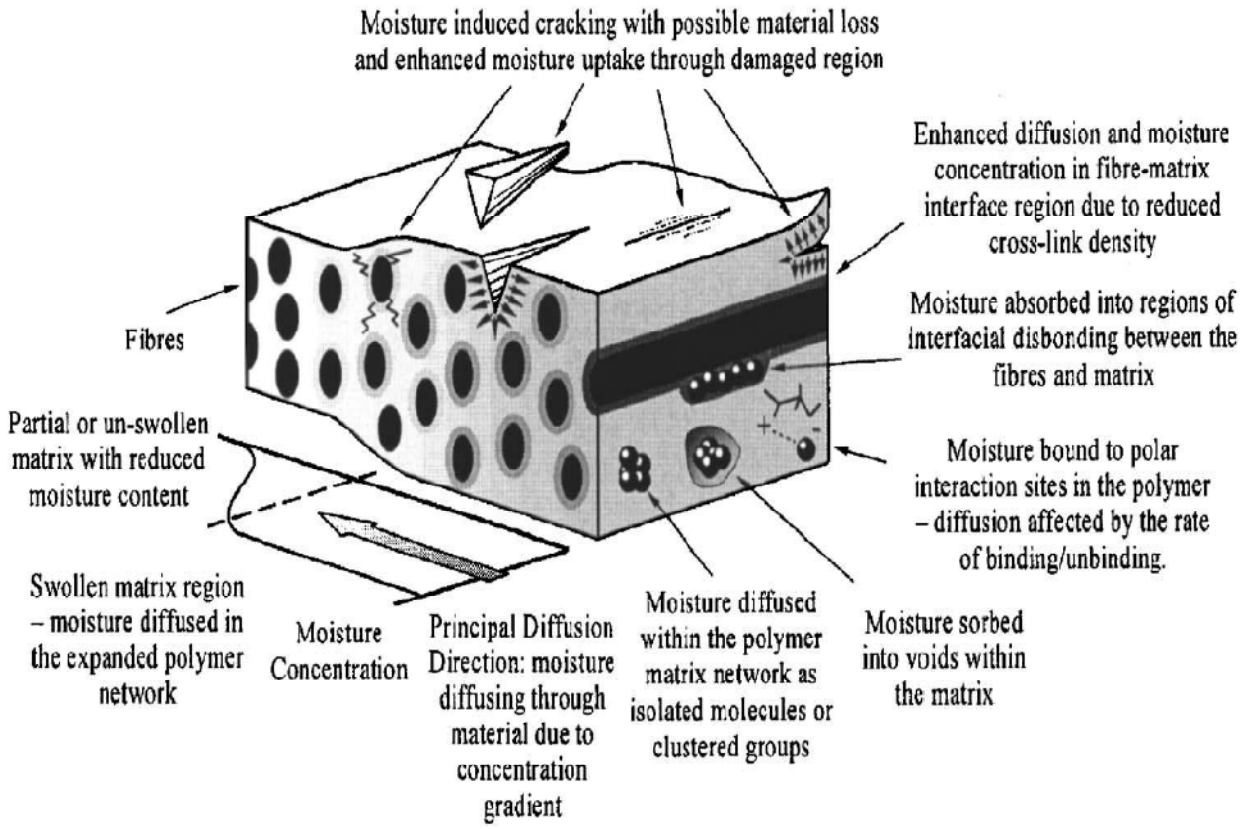

Fig. 1.9 Deteriorated fiber specimens under moist environmental condition

For an undamaged material, well-accepted moisture transportation models are available. The most common models for the transportation of moisture in undamaged polymeric composite materials are Fickian diffusion and Langmuir diffusion. If the material contains cracks that significantly affect the moisture uptake, then the original laws of Fickian and Langmuir are no longer valid for the whole laminate, but locally they still work. The influences of matrix cracks on moisture uptake in glass-fiber/epoxy laminates have been studied. Experiments, finite element calculations and analytical calculations have been performed and the results are compared. The experimental results show that crack closure may occur early in the absorption process and that the crack closure is significantly influencing the moisture absorption.

Wang *et al.* (2001) prepared polymeric nano-composites by melt intercalation method. The nanoclay was mixed with polymer by twin-screw extrusion. The clay-spacing in the composites was measured by X-ray diffraction (XRD). The morphology of the composites and its development during the extrusion process were observed by scanning electron microscopy **(**SEM**).** Melt viscosity and mechanical properties of the composites and the blends were also measured. It was found that the clay spacing in the composites was influenced greatly by the type of polymer used. Also the addition of the nanoclay increased the viscosity of the polymer when there was a strong interaction between the polymer and the nanoclay. The mechanical test showed that the addition of 5-10 wt. % nano-clay largely increased the elastic modulus of the composites. The water absorption of nylon 6 was decreased with the presence of nano-clay. The effect of nano-clay on polymers and polymer blends was also compared with Kaolin clay under the same experimental conditions.

Sinha Ray *et al.* (2003) discussed the academic and industrial aspects of the preparation, characterization, materials properties, crystallization behavior, melt rheology and processing of polymer/layered silicate nanocomposites. Smectites were a valuable mineral class for industrial applications because of their high cation exchange capacities, surface area, surface reactivity, adsorptive properties. These composites exhibited improved mechanical properties compared to conventional composites. The composites exhibited a remarkable increase in thermal stability, as well as self-extinguishing characteristics for flammability, such that the flammability of pristine polymers was significantly reduced after nanocomposite formation with layered silicate.

Chow *et al*. (2005) analysed the water absorption and hygrothermal aging behaviour of organomontmoiillonite (OMMT reinforced polyamide 6/polypropylene (PA6/PP ratio = 70/30), with and without maleated PP (MAH-g-PP), at three different temperatures (30, 60, and 90^{o}C. The water absorption of the PA6/PP nanocomposites obeyed the Fickian law behavior. It was found that the equilibrium moisture content and the diffusion coefficients were dependent on the OMMT loading, MAH-g-PP concentration and immersion temperature tensile modulus and strength of PA6/PP nanocomposites deteriorated after exposure to hygrothermal aging. Water acted as a plasticizer for the PA6/PP matrix and silicate layer of OMMT. The nanocomposites

showed excellent retention ability and recovery properties under any immersion temperature. The MAH-g-pp enhanced the resistance of the nanocomposites against water immersion and also improved the resistance against hygrothermal attack.

Kornmann *et al*. (2005) manufactured epoxy-layered silicate nanocomposites based on anhydride cured epoxy and octadecylamine modified fluorohectorite as matrix in glass-fiber-reinforced laminates by hand lay-up technique. The material used was the synthetic layered silicate Somasif ME-100. One hundred and twenty milli-equivalents per 100 g of Somasif ME-100 of ocadecylamine were dispersed in deionised water at 80^{o}C. They had done the flexural tests on the laminates and indicated that the presence of silicate layers in the epoxy matrix leads to a flexural strength improvement of 27%. According to dynamic mechanical measurements, the presence of organosilicate caused a decrease of the glass transition temperature. The glass transition temperature decrease was apparently responsible for the larger water uptake observed in the nanocomposite.

Lin *et al*. (2005) prepared Layered silicate/glass fiber/epoxy hybrid composites using a vacuum-assisted resin transfer molding (VARTM) process. Unidirectional glass fibers were placed in two directions: parallel and perpendicular to the resin flow direction. The intercalation behavior of the clay and the morphology of the composites were investigated using X-ray diffraction (XRD) and transmission electron microscopy (TEM). The complementary use XRD and TEM techniques revealed an intercalated clay structure in the composites. Dispersion of clay in the composites was also observed using scanning electron microscopy (SEM); the observed clays were dispersed between both the bundles of glass fibers and within the interstices of the fiber filaments. The mechanical properties of the ternary composites were evaluated. The results indicated that introducing a small amount of organoclay to the glass fiber/epoxy composites enhanced their mechanical and thermal properties, confirming the synergistic effects of glass fibers and clays in the composites.

Yasmin *et al.* (2006) prepared the clay/epoxy nanocomposites by shear mixing method and used the 1-10wt. % of clay concentration to prepare the samples. The epoxy matrix was reinforced with MMT clay particles to fabricate clay/epoxy nanocomposites. Bisphenol A was used as epoxy resin and methyl tetrahydrophthalic anhydride as the hardener. Two types of clay nanoparticles were used as the reinforcement, one was Nanomer I.28E and other was Cloisite

30B. In this study Closite 30B showed a homogeneous dispersion of nanoparticles throughout the cross-section compared to Nanomer I.28E. As the clay content was increased, the strain to failure decreased. It was also found that the modulus of the nano-composites increased monotonically with increasing clay content. For 10wt.% of clay, the Cloisite30B/epoxy showed an increase of 53% over the neat resin, where as the other showed an increase of about 22% at room temperature. The observation further confirmed the direct relation between the degree of exfoliation and the mechanical properties of these nanocomposites. The addition of clay also found to reduce the CTE (coefficient of thermal expansion) of pure epoxy.

Avila *et al*. (2006) manufactured a set of fiber glass-epoxy-nanoclay laminate composites to investigate how the plate impact strength is affected by the presence of nanoclays. The S2-glass/epoxy nanoclay composite made was a laminate with 16 layers and 65% fiber volume fraction prepared using a vacuum assisted lay-up technique. The amount of nanoclay added into an epoxy system, in weight, was 1%, 2%, 5%, 10%, respectively. To compare the results, a set of S2-glass/epoxy laminated composites were also prepared. The addition of nano sized clays increased the composite impact strength, as the damaged area was decreased approximately 20% for small amounts of nanoclay contents. When the concentration reached around 10%, the increase on impact strength was near to 50%. Nanoclay composites showed great performance over the conventional composites under the rebound/spring effect. When the four edge clamped condition was imposed the overall composite damping was increased with the nanoclay concentration. The most favourable nanoclay concentration suggested by them was close to be 5%. This could be due to the vibration mode superposition associated to a stiffness enhancement.

Avila *et al.* (2006) investigated the influence of montmorillonite (MMT) silicate layers on glass-fiber-epoxy laminated composites behavior by low-velocity impact and X-ray diffraction tests. The nanostructure laminate prepared for the investigation was a S2-glass/epoxy-nanoclay. The nanoclay used was Nanomer I30E. The amount of nanoclay dispersed into the epoxy system, in weight, was 1%, 2%, 5%, 10%, respectively. As the amount of nanoclay dispersed was increased, there was an increase in stiffness. As the stiffness reached its peak value, the fracture toughness and damping were reduced. Specimens with 5% nanoclay content showed the best performance with respect to damping. As the energy increased, the nanostructure laminate response got weaker. When the low-velocity impact results were analyzed they showed an

increase on energy absorption close to 48% for low energies, 20 J, 15% increase for medium–high energies, 60 J, and 4% for high energy, 80 J. As the amount of intercalated nanoclay content varied from 0% to 10%, the optimum condition for low-velocity impact seemed to be around 5%.

Wetzel *et al*. (2006) analysed the characterization of epoxy nanocomposites. The incorporation of both Al_2O_3 and TiO_2 nanoparticles into the epoxy resin improved flexural stiffness, flexural strength, and fracture toughness of the polymer at the same time. Cracks in Dynamically loaded nanocomposites propagated at lower rates than in neat epoxy. The fillers were well bonded to the matrix, which was indicated by both the shift of the glass transition temperature to higher temperatures and the increase in the rubbery plateau modulus. Moreover, the presence of Al_2O_3 in epoxy increased the apparent yield stress, the yield strain, and the size of the plastic zone. Debonding effects in the process zone, as often observed in glass bead filled epoxies, were rather unlikely to participate in the toughening of EP/Al_2O_3 nanocomposites, due to the small dimensions of fillers. Further investigations would help to find relationships especially between the morphology, the relevant toughening mechanisms, and the toughness of EP/Al_2O_3 nanocomposites. It was believed that the observed property characteristics were related to the influence of nanoparticles on the molecular structure of the matrix itself.

Wang *et al.* (2006) investigated the effects of hydrothermal ageing on the thermo-mechanical properties of high performance epoxy and its nanocomposite. In this work epoxy–clay nanocomposite samples containing 2.5 wt% of clay were prepared through "slurry-compounding" approach. The cured samples were immersed in distilled water at 60°C for different periods of time before subjecting to characterization. The hydrothermal effect on the thermal/mechanical properties of neat epoxy and epoxy–clay nanocomposite was studied. The moisture uptake significantly affects the modulus at high temperature, the tensile strength, and the α-relaxation behavior. On the other hand, at low temperature, the modulus and fracture toughness were not strongly influenced. As the moisture content increased, there was a reduction in strain at break for the epoxy–clay nanocomposite while that of the neat epoxy remained constant. This effect was attributed to epoxy–clay interface debonding induced by water and formation of water cluster fillers that acted as defects in the composite.

Berketis *et al.* (2007) investigated the matrix and fiber/matrix interfacial degradation of glass fiber composites subjected to water for very long time. Laminated composite plates were manufactured by the vacuum assisted resin transfer moulding technique. The resin used was the polyester (crystic 489 PA). The durability of an isopthalic polyester resin reinforced with non-crimp glass fabrics in a hydrothermal environment was studied for up to 30 months. The weight of the composite plates initially increased due to water diffusion up to month 14 and thereafter decreased due to material losses. The initial weight increase was due to diffusion of water into the specimens. Immersion in water also resulted in significant de-bonding of the fiber/matrix interface, which allows water to penetrate the composite material by capillary action. The impacted plates were retested statically to determine residual compressive strengths for the assessment of damage tolerance. A new device was designed for the CAI tests that assured laminate failure by de-lamination propagation. The results of the CAI testing demonstrated a reduction in CAI strength, due to hydrothermal exposure for each applied level of impact loading. Immersion time of 24 and 30 months showed that a local plateau was approached in CAI strength.

Quaresimin *et al*. (2007) analysed the effect of three different commercially available nano-modifiers on the mechanical properties of an epoxy/anhydride unidirectional carbon fiber reinforced laminates. The polymeric matrix consisted of a blend of the diglycidyl ether of Bisphenol A and the epoxy novolac resin. The hardener was a hexa-hydrophthalic anhydride. The nanoclay used was Cloisite 30B. The organoclay was dispersed through a shear mixing process. Hand-layup method was used to prepare the specimens. The tensile modulus exhibited little difference between the unmodified laminates while a modest decrease was observed for the tensile strength for the VGCF (vapors grown carbon fiber) and nanoclay modified systems. The result being that the ‘‘effective’’ clay concentration in the interlayer resin rich regions was much higher than the nominal nano-additive concentration.

Shang-Lin *et al.* (2007) performed experimental investigation of nanocomposite coatings for healing surface flaws of glass fibers and improving alkali-resistance. He found that, with low fraction of nano-reinforcements, the nanostructures and functionalised traditional glass fibers show significantly improved both mechanical properties and environmental corrosion resistance. The most remarkable mechanical strength improvement was found for glass fibers with nanotube

coatings, corresponding to the highest healing efficiency factor. No apparent strength variation appeared for nanoclay coated fiber subjected to alkaline attack, which indicated that, the influence of moisture solvent uptake and concentration on mechanical properties decreased when the organoclay was dispersed in coating polymer. Overall, the hybrid nanocoatings caused improved fiber strength, corrosion resistance, and interfacial properties.

Chow *et al. (2007)* prepared the epoxy/glass fiber/organo-montmorillonite (OMMT) nanocomposites by hand lay-up method. In this work, the epoxy nanocomposites were characterized by X-ray diffraction (XRD), differential scanning calorimetry (DSC) and water absorption tests. Epoxy/glass fiber/OMMT hybrid nanocomposites prepared by hand-layup technique showed exfoliation characteristics and slightly enhancement in glass transition temperature. The water resistance properties of epoxy were improved by the addition of both glass fiber and OMMT, which is may be attributed to the increasing of the tortuosity path for water penetration.

Manjunatha *et al*. (2009) investigated the tensile fatigue behavior of a silica nanoparticle-modified glass fiber reinforced epoxy composite. The epoxy resin was a standard diglycidyl of Bisphenol A with an epoxide. The GFRP composite laminates were manufactured by resin infusion under flexible tooling technique. An anhydride-cured thermosetting epoxy polymer was modified by incorporating 10 wt. % of well-dispersed silica nanoparticles. The fatigue life of 10 wt. % silica nanoparticle-modified bulk epoxy was about three to four times higher than that of neat epoxy. The fatigue life of the GFRP composite with 10 wt. % silica nanoparticle modified epoxy matrix was about three to four times higher than that of the GFRP with the neat epoxy matrix. The suppressed matrix cracking and reduced crack growth rate due to the particle debonding and plastic void growth mechanisms appeared to contribute for the observed enhancement of the fatigue life in the GFRP with the nanoparticle-modified matrix.

Maitra *et al*. (2009) synthesized and evaluated PVA polymer-matrix composites reinforced with small concentrations of functionalized ND. Detailed structural characterization, employing a variety of analytical techniques, showed that the nanoparticles were distributed uniformly and did not agglomerate. Further, they appeared to interact with the polymer matrix strongly, increasing the crystallinity substantially. The mechanical properties of the PVA-ND composites were determined using nano-indentation technique. With only 0.6-wt% addition of ND, which

was relatively small, significant enhancements to the hardness and Young's modulus of the PVA were observed. It was suggested that excellent adhesion between the matrix and the functionalized ND particles was the main reason for this marked improvement in mechanical performance. These results indicated that ND could be successfully used as a filler material for making polymer composites.

Zainuddin *et al*. (2010) analysed the effect of environmental conditioning especially under hot-wet conditions on E-glass epoxy fiber reinforced composite. The weight gain was higher for all the wet conditions samples exposed to elevated temperatures. Addition of 1–2 wt% of nanoclay decreased the weight gain. Flexural properties were found to degrade with increase in time. 2 wt% GFRP composites showed enhancement in properties under all conditions over neat counterparts. In some cases, samples subjected to hot dry condition at 60^0C showed increase in properties over room temperature conditioned samples. Scanning electron micrographs provided clear evidence of the effects of nanoclay, elevated temperature and moisture absorption. Enhancement in interfacial bonding was observed in 2wt. % composite samples, both at room temperature and hot-wet conditioning.

Hossain *et al*. (2011) investigated the effect of seawater on the degradation of mechanical properties of conventional and nanophased carbon-epoxy composites. Epoxy resin was modified using 1 wt. %, 2 wt. %, and 3 wt. % nanoclay. Carbon-epoxy composites were fabricated by vacuum assisted resin transfer moulding process and compared with neat samples with and without exposure to seawater. Nanoclay was dispersed into matrix by using magnetic stirring. Mechanical characterization performed through three point bending tests showed that 2 wt. % nanoclay loading was optimum. Flexural strength and modulus were increased by 25% and 12.51%, respectively, compared to neat system for samples not exposed to seawater. Flexure samples exposed to the seawater for 30, 60, and 180-day periods revealed that samples with nanoclay retained better mechanical properties compared to neat samples. After 30-day exposure to seawater, there was no significant reduction in the strength and modulus. However, flexural strength was reduced by 10.24%, 7.08%, 5.28%, and 7.13% for neat, 1 wt.%, 2 wt.%, and 3 wt.% nanoclay-infused samples, respectively, after the samples were exposed to seawater for 180-day. At the same time flexural modulus was reduced by 12.61%, 7.16%, 4.59%, and 6.11%, respectively. From scanning electron microscopy (SEM) studies, it was found that failure

occurred due to delimitation and initiated from the compression side. Nanophased composites exhibited better bonding between fiber and matrix. SEM micrographs also revealed that both unconditioned and conditioned nanophased epoxy, which produce relatively rougher fracture surfaces compared to neat samples. Optical microscopy study revealed no significant physical change in outer surfaces of the samples conditioned up to a 90-day period.

Zafar *et al*. (2012) investigated the long term effects of moisture on the interface between a carbon fiber and an epoxy matrix. High modulus carbon fibers were used to prepare single fiber model composites based on an epoxy resin. The samples were immersed in the seawater and demineralised water and their moisture uptake behaviour was monitored. The equilibrium moisture content and diffusion coefficients for the samples were determined. DSC (Differential scanning calorimetry) had been used to analyse the moisture effects on glass transition temperature and thermal stability of the pure epoxy specimens. These results showed a reduction in the glass transition temperature (Tg) after moisture absorption. Tensile tests were also carried out for the epoxy specimens and a general decrease in the mechanical properties of the epoxy matrix was observed. Raman spectroscopy was used to observe the effects of moisture on the axial strain of the carbon fiber within the composite and stress transfer at the interface as a function of exposure time. The results show that the decrease in the mechanical and interfacial properties of the model composites under the seawater immersion is more significant than under demineralised water immersion

CHAPTER 3 RESEARCH PROBLEM

3.1 Gaps in literature

From the literature review it is found that previous work has mainly focused on the synthesis of neat epoxy based FRP's and the characterization of the mechanical properties. There are very few publications on the hygrothermal aging studies of these FRP's. Some of the following gaps are there in the previous research.

1. There are still difficulties in dispersing reinforcing particles at nano-scale homogeneously in the matrix.
2. Effect of varying nanoclay concentration on thermal stability of FRP laminated nanocomposites does not show consistent results.
3. No report on the hygrothermal aging studies of these nanocomposites with different fiber stacking sequences.

3.2 Research problem

The present study will mainly focus upon the synthesis of epoxy layered silicate nanocomposites as matrix in fiber reinforced composites. In this study, mechanical properties and thermal stability of these FRP laminated nanocomposites with different stacking sequence would be studied. It is also proposed to carry out some hygrothermal aging studies on these FRPs.

CHAPTER 4 EXPERIMENTATION

4.1. Fabrication of specimen

4.1.1. Materials

Unidirectional E-glass fiber and M Brace a two part epoxy resin purchased from BASF Construction Chemicals (India) Private Limited. Organically modified nanoclay Closite 30B purchased from Connell Bros. Mumbai.

4.1.2. Specimen specifications

Commercially available glass fiber mat had been used for making specimen. The sheets were placed along 0^0 orientation side for cutting the specimen. The specimen had been cut and prepared as per the assumed dimensions for tensile and bending tests respectively. The assumed dimensions of specimens are shown below.

Table 4.1 Specimen specifications for testing

Parameters for specimen	**Specimens for tensile testing**	**Specimens for flexural testing**
Length	125 mm	125 mm
Width	15 mm	13 mm
Thickness	3 mm	3 mm

4.1.2.1. Specimen dimensions

- **For bending test**

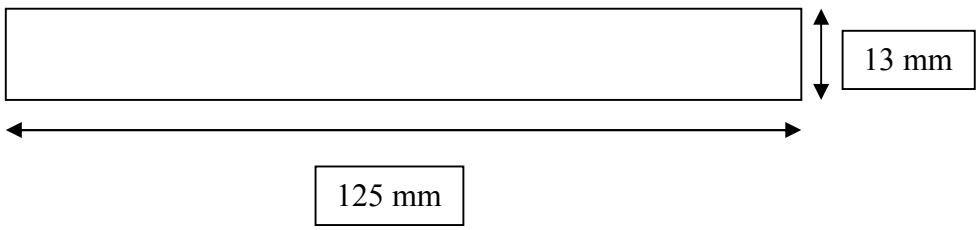

Fig.4.1 Specimen dimensions for bending test

- **For tensile test**

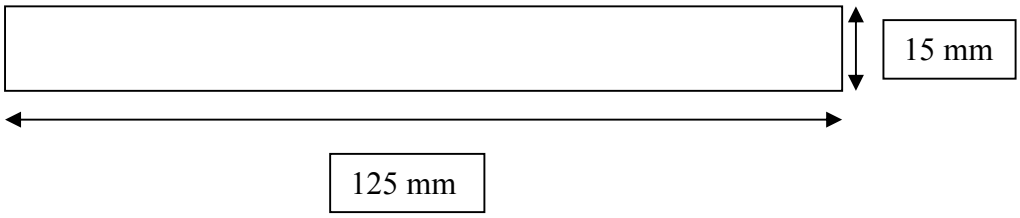

Fig.4.2 Specimen dimensions for tensile test

4.1.3. Cutting glass fiber sheet

For the experimentation, unidirectional roll of glass fiber was purchased having 50cm width having 0^0 fiber orientation woven with polymer fibers. The sheets were initially cut from roll in lengths of 500 mm (Fig. 4.3).

Fig. 4.3 Uncoated glass fiber mat used for making specimen

4.1.4. Mixing of nanoclay into epoxy (base):

- **Mechanical stirring**: Epoxy base is a blue colour thick fluid. It is quite difficult to mix nano silicates into it manually. So we used a mechanical stirrer and an oil bath for proper mixing of nanoclay (Fig. 4.4). Oil bath was used to heat up the epoxy to desired (60^0C) temperature, so the viscosity of epoxy base is reduced. Proper mechanical stirring of epoxy at this stage resulted better dispersion of clay.

Fig. 4.4 Oil bath set-up with mechanical stirrer

Different weight percentages of clay – 0.5, 2, 3 and 4 % by weight of epoxy, were added and stirred at a temperature of 60^0C for 2 hours.

- **Ultrasonication after mechanical stirring**: Sonication is the act of applying sound energy to agitate particles in a sample, for various purposes. In the laboratory, it is usually carried out using an ultrasonic bath or an ultrasonic probe, colloquially known as a sonicator. Sonication can be used to speed dissolution, by breaking intermolecular interactions. Sonication was done for evenly dispersing nanoparticles in liquids. After mechanical stirring of the epoxy solution container was placed into the ultrasonication bath for up to 2 hours.

Fig.4.5: Ultrasonication bath

4.1.5 Mixing of epoxy base solution with hardener:

After ultrasonication, the solution is mixed with the hardener in the ratio 10:4 by volume. After mixing, mechanical stirring up to 5 to 10 minutes was done. The whole procedure is shown in Fig. 4.6.

Fig. 4.6 Mixing of hardener to the base component

4.1.6. Coating of nanoclay mixed epoxy to glass fiber sheets:

The mixture was then poured on to the glass fiber mat and applied uniformly using the hand layup method. For this, steel scraper was used to maintain uniformity of the solution. It was made sure that there is no air bubbles entrapped inside the epoxy applied on sheet otherwise it would create a flaw there. After applying epoxy on the both sides of first glass fiber, second fiber sheet was applied on first fiber sheet with 90^0 orientation with respect to first fiber sheet and epoxy was applied on second fiber sheet. Finally third fiber sheet was placed on second fiber sheet with 0^0 orientation with respect to first fiber sheet and epoxy was applied on third fiber sheet. The sheet took overnight to dry. The full curing of sheet (Fig. 4.7 & Fig. 4.8) was done by leaving it under ambient temperature for at least seven days before processing further.

Fig. 4.7 Coating the glass fiber sheet with epoxy solution

Fig. 4.8 Coated sheets placed for curing

4.1.7. Cutting of sheet for samples

Once the epoxy was fully cured, cut the sheet to actual sample size using the marble cutter (Fig. 4.9).

Fig. 4.9 Marble cutter

4.2. Experimental set-up

A set of accelerated aging tests had been carried out to evaluate performance of glass fiber reinforced polymer (GFRP) sheets embedded in epoxy matrix. The field environment very similar to that of tropical climate had been simulated. The specimens were immersed in two water baths for different time durations. The specimens were removed from the bath after an interval of 30 days. The tensile and flexural strength was measured to check the degradation in properties of composite material. Both of the water tanks were filled with water. One was of simple water and other tank was containing NaOH 5% by weight of water. Both the tanks were kept at a temperature of 45^0C.

Fig. 4.10 Setup view of the water baths

4.2.1. Setup fabrication

Table 4.2 Shows that the set-up basically consists of following main items

S.No.	ITEM NAME	QUANTITY
1	Water tanks	02
2	Specimens	16
3	Heating Elements	02
4	RTD Sensors	02
5	Temperature Controllers	02

4.2.2. Water tanks

The experimental setup consists of two well insulated tanks (Fig. 4.10). The tank was of cylindrical shape made out of plastic. The approximate capacity of the tank was 60 liters. Both the tanks were filled totally with tap water and set at a temperature of 45°C. NaOH was added to one tank (5% by weight of water). The water which evaporated from the tank was replenished on daily basis during experimentation. Each tank was labelled as per details of experimentation.

4.2.3. Heating element

The setup was heated with help of commercially available heating rod elements (Fig. 4.11). Each bath was having its own heating rod connected via temperature controller (Fig.4.12). The wattage of rod was 1000KW with single phase connection. As the temperature reached the required value the power supply of rods were cut off by controllers.

Fig. 4.11 Heating element and RTD sensor in a tank

4.2.5. Temperature controller

The objective of this set up was to maintain the bath temperature at specified value till the duration of experiment for day and night on daily basis. So a temperature controller (Fig.4.12) was connected with each of the bath along with relays cut off. The controller used the proportional-integral-derivative (PID) control to maintain the temperature. On the controller display the “Set Value” was given which was the temperature indicated in green and the “Process Value” of temperature was indicated in the red (refer Fig.4.12), which was the output from the RTD sensor. For the very first time the controller was set to auto-tune mode so that it could adjust itself according to the input variables. Once the bath had attained the set value the controller cut off its supply and after sometime it sensed the temperature if it had gone below set value, it again started heating to obtain the set value. The dimensions of the controller and actual panel used are shown in Fig.4.12 and Fig. 4.13 respectively.

Fig. 4.12 Temperature controller **Fig. 4.13 Temperature display panel with controller**

4.3. Testing methods used in experimentation

4.3.1. Tensile testing

A Universal tensile testing machine shown in Fig.4.14 and Fig.4.15 was used for the testing of the FRP specimen for its tensile strength. The test specimen had been prepared according to assumed dimensions. The specimen were tested until they break indicating the peak load and ultimate stress value they can bear at required time period to estimate the degradation in the same machine.

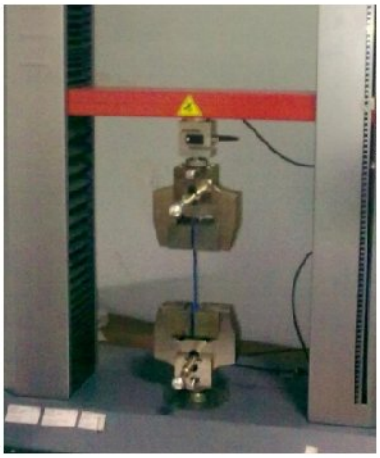

Fig. 4.14 UTM testing machine **Fig. 4.15 Specimen in jaws**

4.3.2. Three point flexural test

Three point bending tests of specimen were carried out in using Zwick/Roell (Fig. 4.16 & Fig. 4.17).

Fig. 4.16 Three point bend test machine

Fig. 4.17 Specimen positioning

The test specimen had been prepared according to assumed dimensions. The three point bending test results can be taken as indications of strength degradation of composites after they had been hygrothermally treated.

4.3.3. Micro hardness test

Micro hardness test (shown in Fig.4.18) was conducted on specimen with different clay loadings to see the effect of clay loading on hardness values.

Fig. 4.18 Micro hardness equipment

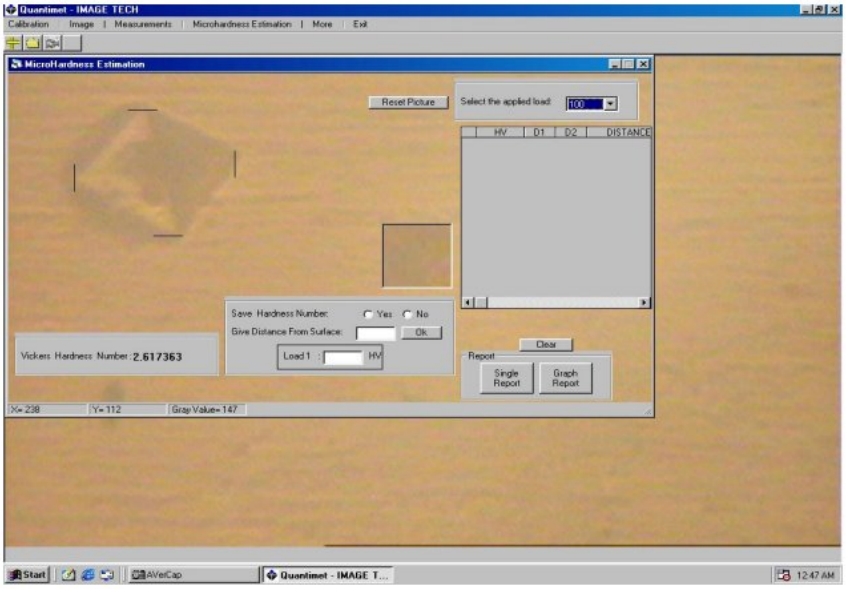

Fig. 4.19 Indent of specimen

The load applied was 50gm and VHN values were determined by applying this load by using a calibration distance of 50 units in Quantinet software as shown in Fig.4.19 used for image analyzing. The dwell time used during load application was 20 seconds. An indent is formed in diamond shape used for calculating VHN as shown in figure below.

4.3.6. X-Ray diffraction test

X-ray scattering techniques are a family of non-destructive analytical techniques which reveal information about the crystallographic structure, chemical composition, and physical properties of materials and thin films. These techniques are based on observing the scattered intensity of an X-ray beam hitting a sample as a function of incident and scattered angle, polarization, and wavelength or energy.

X-ray diffraction was used in this study to investigate the crystallographic structure of the epoxy nanocomposites. XRD will enable the changes that occur to the clay due to the intercalation and/or exfoliation of the epoxy into the clay galleries to be quantified. The d-spacing of the intergallery spacing can be determined using Bragg‟s Law:

$$\lambda = 2d\sin\theta$$

Where λ is the wavelength of the incidence x-ray source, d is the spacing in question, θ is ½ of 2θ the Bragg angle or the diffracted angle of the incidence x-ray beam. Below is a schematic of the previously mentioned Bragg's Law (Fig. 4.20).

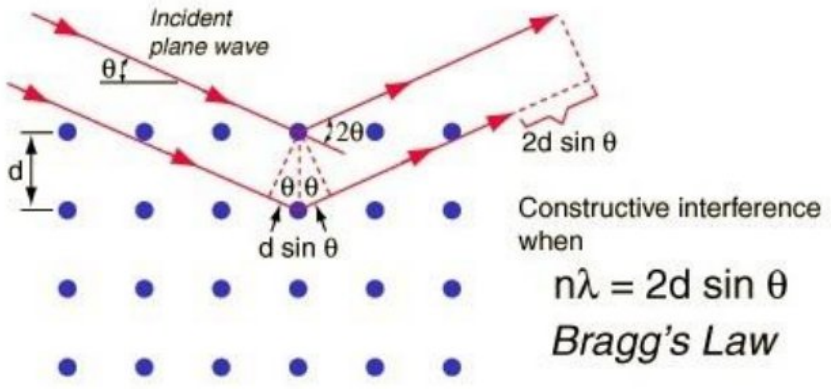

Fig. 4.20 Schematic representation of x-ray diffraction principle and the Bragg's Law

To evaluate the degree of exfoliation in the polymer, XRD measurements were carried out in a Panalytical X-ray diffractometer with Cu Kα radiation (λ=1.54Å) with a scanning speed of 10/min and at 45 kV and 40mA. During the XRD experiments, the samples were analyzed in reflection mode. All XRD scans were through 2θ of 5^0 to 15^0.

4.4. Test matrices

Table 4.3 Initial testing specimens

Specimen Name	**No. of specimens**		**Total specimens**
	Tensile	**bending**	
0 wt%	3	3	6
0.5 wt%	3	3	6
2 wt%	3	3	6
3 wt%	3	3	6
4 wt%	3	3	6
Total specimens			**30**

Table 4.4 Distribution of above GFRP nanocomposite specimen for accelerated degradation in 45°C simple water bath

Specimen name	No. of specimens		Total specimens
	Tensile	bending	
0 wt%	2	2	4
0.5 wt%	2	2	4
2 wt%	2	2	4
3 wt%	2	2	4
4 wt%	2	2	4
Total specimens			**20**

Table 4.5 Distribution of above GFRP nanocomposite specimen for accelerated degradation in 45°c NaOH solution (5% by weight of water)

Specimen name	No. of specimens		Total specimens
	Tensile	bending	
0 wt%	2	2	4
0.5 wt%	2	2	4
2 wt%	2	2	4
3 wt%	2	2	4
4 wt%	2	2	4
Total specimens			**20**

5.1 MICROSCOPIC BEHAVIOR

5.1.1 Micro-Hardness

5.1.1.1 Specimen for micro hardness

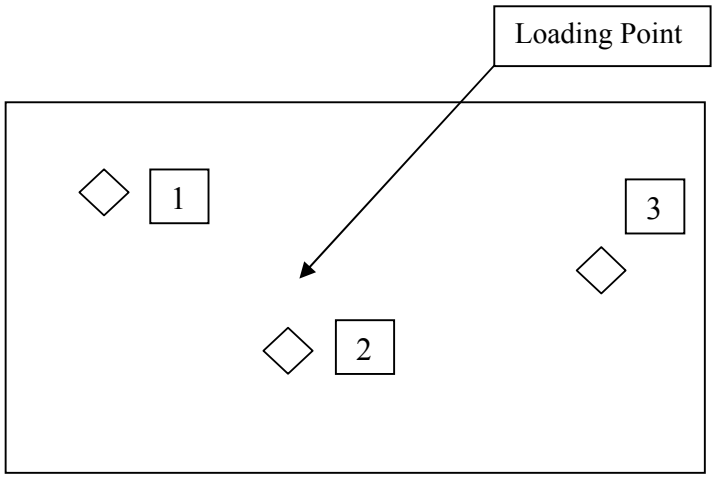

Fig. 5.1 Location of loading points in specimen

The micro-hardness of specimen manufactured at different clay loading was measured. The table 5.1 shows the experimental observations of the nanocomposites with different nanoclay contents. An average hardness was calculated by taking measurements at 3 points in each specimen. Fig 5.2 shows the results of Vickers hardness plotted against nanoclay loading.

Table 5.1 Micro hardness values for different clay loading specimens

Clay Loading → / Loading Points ↓	Micro hardness values				
	0 wt%	**0.5 wt%**	**2 wt%**	**3 wt%**	**4 wt%**
Point 1	4.554	6.957	7.281	5.621	5.504
Point 2	4.167	6.079	8.167	4.435	6.235
Point 3	4.203	6.079	7.157	5.789	6.032
Average	**4.308**	**6.372**	**7.535**	**5.282**	**5.927**

The maximum hardness has been measured where the nanoclay content reached 2 wt%. A decline of the hardness also appears on further increasing the nanoclay content. The hardness decreases in a significant manner from 7.535 HV (2 wt% of nanoclay) to 5.282 HV (3 wt% of nanoclay). Thus, adding a small amount of nanoclays into polymer-based materials could potentially enhance hardness of the material with the nanoclay content less than 5 wt%. However, it is also reasonable to believe that it should have an optimal limit depending on choice of constituent material and processing conditions .It was suspected that the nanoclays might retard the chemical reaction, and so cause incomplete curing process of the composites. For all specimens with high nanoclay content, the matrix might not be fully cured.

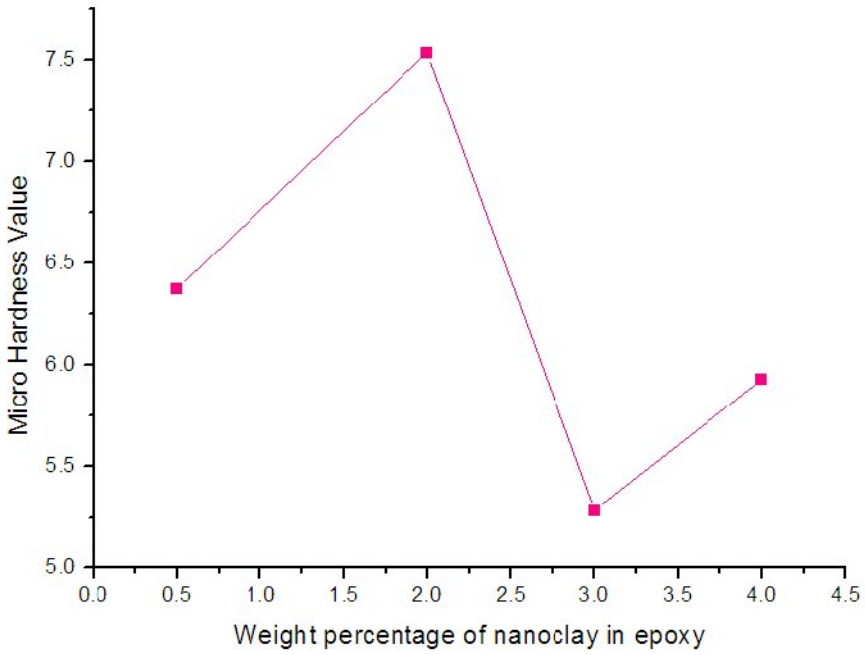

Fig. 5.2 The Vickers' hardness value of specimen as a function of weight percentage of nanoclay in epoxy

5.1.2 X-ray diffraction test

The X-ray Diffraction experiments were conducted on the specimens having different nanoclay loading. X-ray diffractometer gives the values of d-spacing and 2θ for different specimens of epoxy clay nanocomposites. An increase of the interlayer distance leads to a shift of the diffraction peak toward lower angle. The diffraction peak of Closite 30B comes out at an angle 2θ = 4.8452 and corresponding d-spacing value is d = 18.26854.

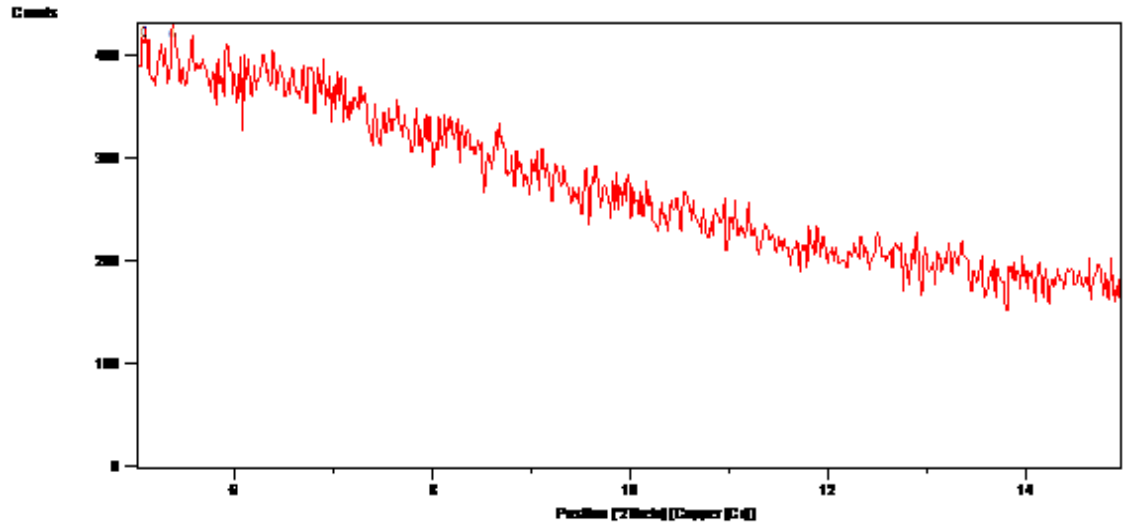

Fig. 5.3 XRD result of specimen with 0.5% clay

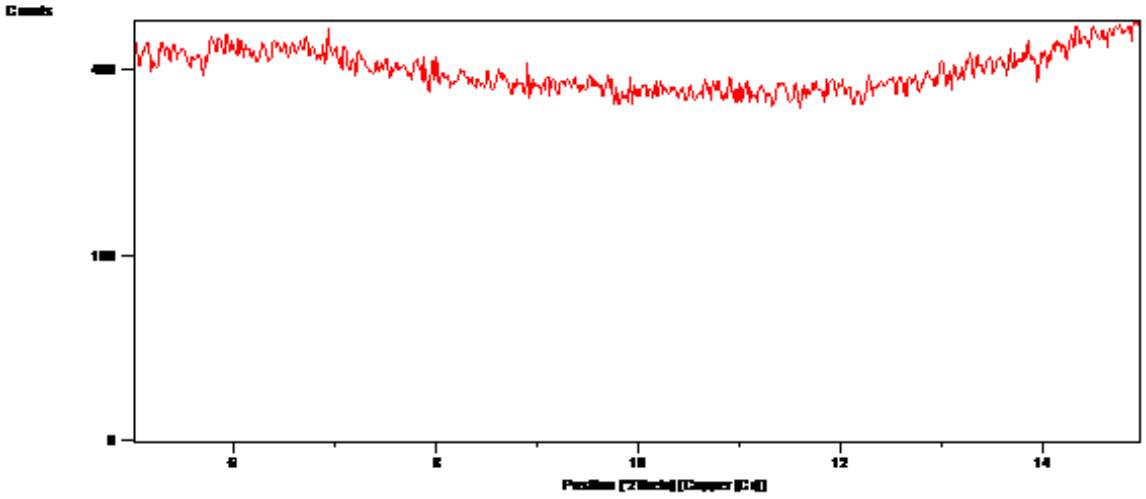

Fig. 5.4 XRD result of specimen with 2% clay

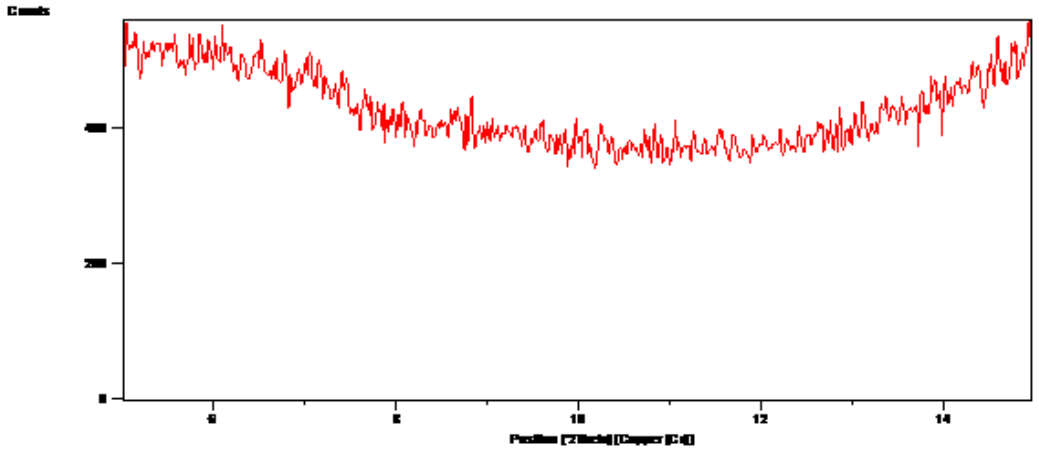

Fig. 5.5 XRD result of specimen with 3% clay

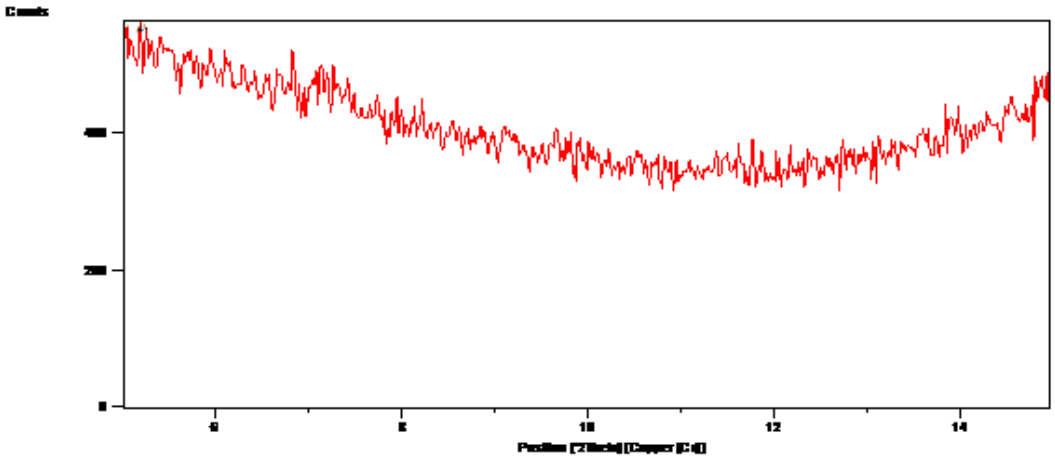

Fig. 5.6 XRD result of specimen with 4% clay

The absence of peaks in diffraction pattern indicated formation of exfoliated nanocomposites at all levels of nanoclay loading.

5.2 Tensile test

The results obtained by conducting tensile tests on nanocomposites using Zwick/Roell universal testing machine are shown in table 5.2.

Table 5.2 Results of specimens from tensile test

Specimen Name	Specimen No.	Tensile Modulus (MPa)	Tensile Strength(MPa)	Strain At Tensile Strength %
0wt%	**Specimen no. 1**	1130	69.0	1.81
	Specimen no. 2	2270	98.2	1.73
0.5wt%	**Specimen no. 1**	474	109	2.21
	Specimen no. 2	964	72.7	1.77
2wt%	**Specimen no. 1**	535	97.8	2.24
	Specimen no. 2	838	72.7	1.97
3wt%	**Specimen no. 1**	1730	109	1.72
	Specimen no. 2	1810	105	2.28
4wt%	**Specimen no. 1**	1500	106	1.76
	Specimen no. 2	520	86.2	1.98

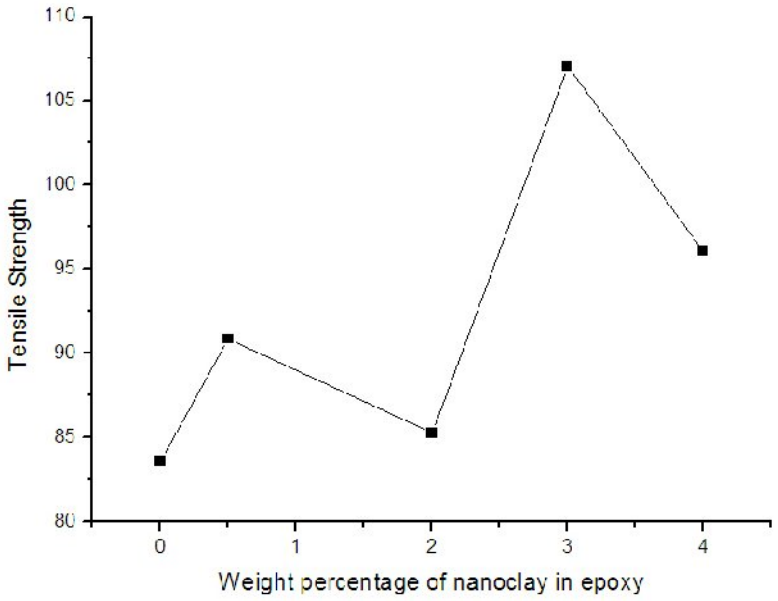

Fig. 5.7 The tensile strength of specimens as a function of weight percentage of nanoclay in epoxy.

The fiber reinforced epoxy nanocomposite specimen having 3wt% nanoclay loading shows the highest value of tensile strength which is 27% higher than neat epoxy glass fiber reinforced composite. The increase in the strength of the epoxy samples must be due to the introduction of nanoclay, which hindered the molecular movement of polymer chains. However, the reason for the sudden drop in the ultimate tensile strength in 2wt% nanoclay was unknown. The variation of ultimate tensile strength as a function of weight percentage of nanoclay in epoxy from 0wt% to 4wt% is shown in Figure 5.7.

5.3 3-point bending test

The results obtained by conducting 3-Point bending tests on nanocomposites using Zwick/Roell universal testing machine are shown in table 5.2.

Table 5.3 Results of specimens from 3-point bending test

Specimen Name	Specimen No.	Elastic Modulus (GPa)	Flexural Strength (MPa)	Deformation At Max. Force %
0wt%	**Specimen no. 1**	0.715	81.7	1.5
	Specimen no. 2	0.662	72.71	1.7
0.5wt%	**Specimen no. 1**	5.96	105	1.6
	Specimen no. 2	3.95	66.5	1.6
2wt%	**Specimen no. 1**	4.43	102	1.9
	Specimen no. 2	3.50	95.1	1.6
3wt%	**Specimen no. 1**	7.02	114	1.6
	Specimen no. 2	6.52	97.7	1.2
4wt%	**Specimen no. 1**	3.90	72.6	2.8
	Specimen no. 2	4.63	85.4	2.1

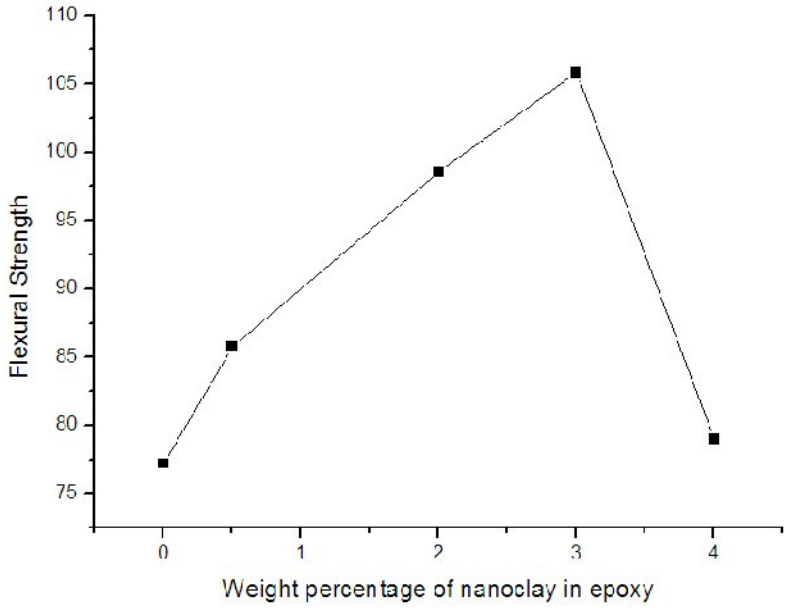

Fig. 5.8 The flexural strength of samples as a function of weight percentage of nanoclay in epoxy.

The addition of nanoclay upto 3wt% results in increase in flexural strength of specimen. A 37% improvement in strength of specimen with 3wt% clay loading is observed when compared with neat epoxy-glass composites. With further increase in nanoclay loading, the strength reduces significantly. The enhancement in the flexural properties could be attributed to the improved interfacial properties responsible for transfer of stresses and elastic deformation in the presence of clay nanoparticles. The results are in accordance with the research carried out by Wetzel *et al.* The flexural strength of a continuous glass fiber composite depends mainly on the compressive strength of fibres because failure usually starts at the compressive side as a result of significantly lower strength in compression than in tension The results are in accordance with the research carried out by Ohsawa *et al.* The presence of nanoclay in the epoxy matrix strengthens and stiffens the surrounding matrix, effectively increasing the compressive strength of the composite. The detrimental effect on strength of clay content higher than 3wt% may arise due to the fibre-matrix interfacial adhesion, which has a significant influence on the composites strength. The flexural strength of samples against the weight percentage of nanoclay in epoxy from 0wt% to 4wt% is shown in Figure 5.8.

5.4.1 Tensile testing results of the specimen under hygrothermal loading

Table 5.4 & 5.5 shows the tensile testing results of the samples immersed in water and NaOH for 0 & 30 days.

Table 5.4 Degradation of nanocomposites in water tank at 45^0C

Water Tank at 45^0C						
No. of Days	**Specimen Name**	**Specimen No.**	**Tensile Modulus (MPa)**	**Tensile Strength(MPa)**	**Strain At Tensile Strength (%)**	**% Decrease in Strength**
0 Day	**0wt%**	**Specimen no. 1**	1130	69.0	1.81	
		Specimen no. 2	2270	98.2	1.73	
	0.5wt%	**Specimen no. 1**	474	109	2.21	
		Specimen no. 2	964	72.7	1.77	
	2wt%	**Specimen no. 1**	535	97.8	2.24	
		Specimen no. 2	838	72.7	1.97	
	3wt%	**Specimen no. 1**	1730	109	1.72	
		Specimen no. 2	1810	105	2.28	
	4wt%	**Specimen no. 1**	1500	106	1.76	
		Specimen no. 2	520	86.2	1.98	
30 Days	**0wt%**	**Specimen no. 1**	1100	73.2	2.11	**2.87**
		Specimen no. 2	464	89.2	2.53	
	0.5wt%	**Specimen no. 1**	1460	90.75	1.67	**4.51**
		Specimen no. 2	500	82.75	2.03	
	2wt%	**Specimen no. 1**	248	76.02	2.84	**2.69**
		Specimen no. 2	1950	89.9	1.98	
	3wt%	**Specimen no. 1**	2090	109	1.63	**6.17**
		Specimen no. 2	6790	91.8	1.12	
	4wt%	**Specimen no. 1**	950	96.8	1.97	**5.52**
		Specimen no. 2	2600	84.8	1.38	

Table 5.5 Degradation of nanocomposites in NaOH tank at 45^0C

NaOH at 45^0C						
No. of Days	**Specimen Name**	**Specimen No.**	**Tensile Modulus (MPa)**	**Tensile Strength(MPa)**	**Strain At Tensile Strength %**	**% Decrease in Strength**
0 Day	**0wt%**	**Specimen no. 1**	1130	69.0	1.81	
		Specimen no. 2	2270	98.2	1.73	
	0.5wt%	**Specimen no. 1**	474	109	2.21	
		Specimen no. 2	964	72.7	1.77	
	2wt%	**Specimen no. 1**	535	97.8	2.24	
		Specimen no. 2	838	72.7	1.97	
	3wt%	**Specimen no. 1**	1730	109		
		Specimen no. 2	1810	105	2.28	
	4wt%	**Specimen no. 1**	1500	106	1.76	
		Specimen no. 2	520	86.2	1.98	
30 Days	**0wt%**	**Specimen no. 1**	518	9.46	0.712	**88.06**
		Specimen no. 2	547	10.5	0.769	
	0.5wt%	**Specimen no. 1**	418	4.07	0.499	**91.65**
		Specimen no. 2	1030	11.1	0.490	
	2wt%	**Specimen no. 1**	473	7.31	0.858	**91.32**
		Specimen no. 2	509	7.48	0.575	
	3wt%	**Specimen no. 1**	1370	11.7	0.472	**90.91**
		Specimen no. 2	957	7.75	0.506	
	4wt%	**Specimen no. 1**	663	9.61	0.730	**88.81**
		Specimen no. 2	643	11.9	0.521	

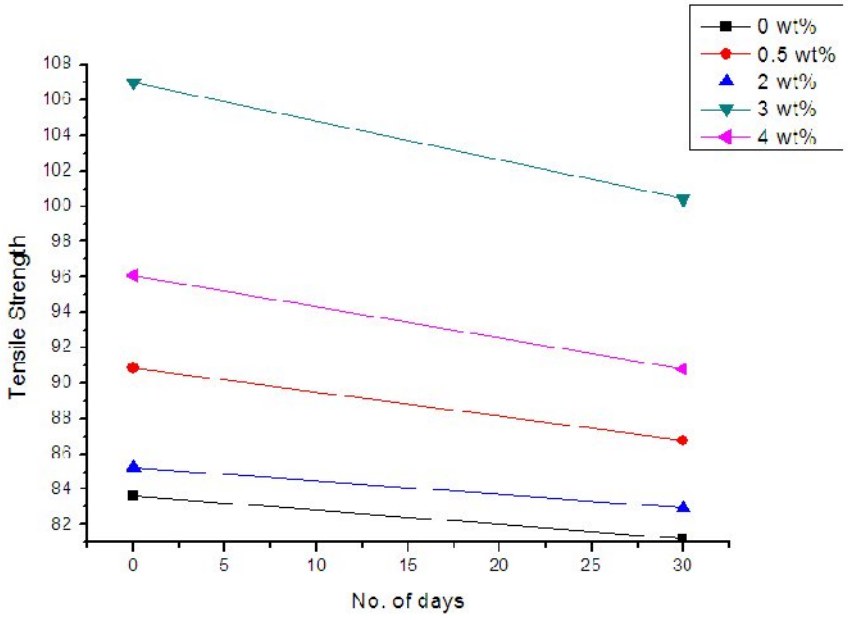

Fig. 5.9 Tensile strength degradation (Water bath at 45^0C)

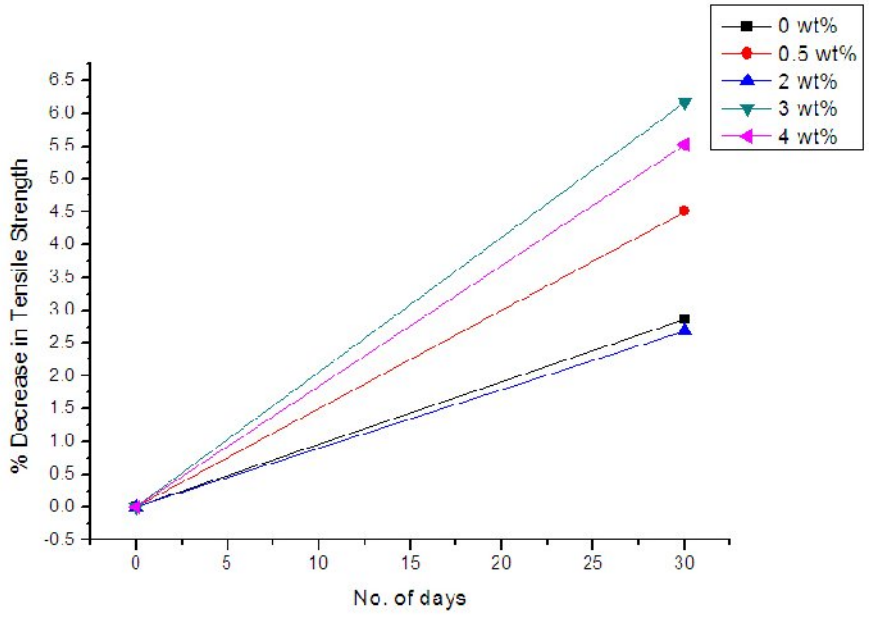

Fig. 5.10 Percent decrease in tensile strength (Water bath at 45^0C)

After 30 days of water immersion of these specimens, there is sharp decrease in tensile strength. The percent decrease in tensile strength value of specimen having 3 wt% of nanoclay loading is highest among other specimens when compared with specimens without water immersion. Figure 5.10 shows the effect of water immersion of specimen on tensile strength. A decrease in strength of all specimens is observed. This may be attributed to the capability of the water molecules to penetrate through the epoxy network. The diffusion of water occurs in epoxy resin was attributed to the nature of the polymer which showed strong interaction with water. In epoxy matrices, water molecules couple strongly with hydrophilic functional groups such as hydroxyl or amine in epoxy resin. The water molecules might interact with epoxy molecules by forming hydrogen bonding with hydrophilic groups. The results are in accordance with the research carried out by Zhou *et al.* The absorption of water could be attributed to the affinity of the functional groups of the epoxies which having high polarity towards water molecules. The results are in accordance with the research carried out by Karad *et al.*

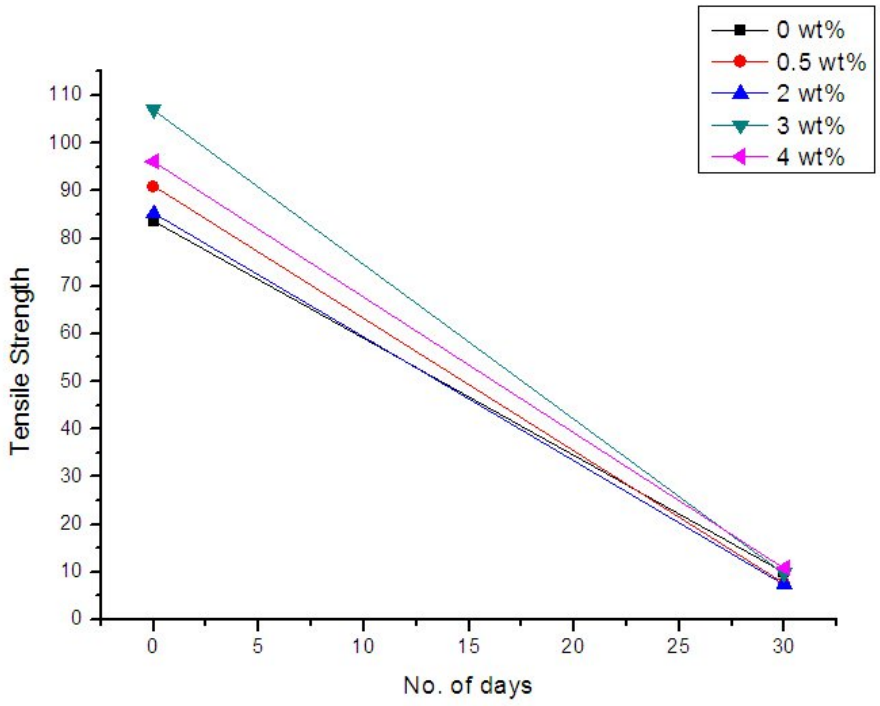

Fig. 5.11 Tensile strength degradation (NaOH bath at 45^0C)

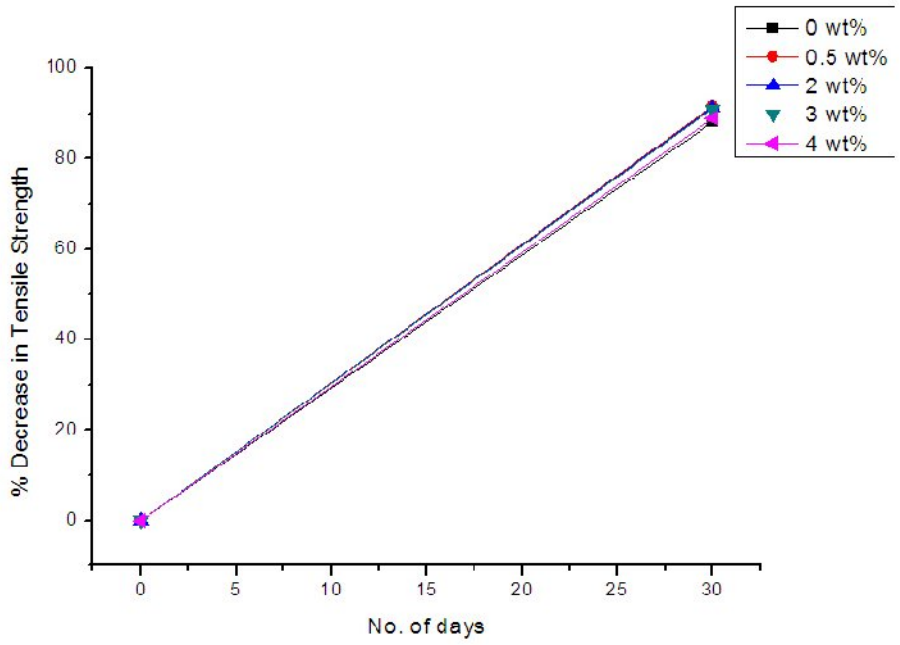

Fig. 5.12 Percent decrease in tensile strength (NaOH bath at 45^0C)

It is also seen that the strength degradation in specimens immersed in NaOH bath was more severe than samples immersed in simple water. A graph of percent decrease in tensile strength and tensile strength degradation as a function of no. of days is shown in Figure 5.11 & 5.12.

5.4.2 Bending test results of the specimens under hygrothermal loading

Table 5.4 & 5.5 showed the bending test results of the samples immersed in water and NaOH for 0 & 30 days.

Table 5.6 Results of specimens for water bath at 45^0C

Water Tank at 45^0C						
No. of Days	**Sample Name**	**Sample No.**	**Elastic Modulus (GPa)**	**Flexural Strength (MPa)**	**Deformation At Max. Force %**	**% Decrease in Strength**
0 Day	**0wt%**	**Specimen no. 1**	0.715	81.7	1.5	
		Specimen no. 2	0.662	72.71	1.7	
	0.5wt%	**Specimen no. 1**	5.96	105	1.6	
		Specimen no. 2	3.95	66.5	1.6	
	2wt%	**Specimen no. 1**	4.43	102	1.9	
		Specimen no. 2	3.50	95.1	1.6	
	3wt%	**Specimen no. 1**	7.02	114	1.6	
		Specimen no. 2	6.52	97.7	1.2	
	4wt%	**Specimen no. 1**	3.90	72.6	2.8	
		Specimen no. 2	4.63	85.4	2.1	
30 Days	**0wt%**	**Specimen no. 1**	0.192	35.3	2.4	**59.26**
		Specimen no. 2	0.187	27.6	2.9	
	0.5wt%	**Specimen no. 1**	1.43	42.5	2.4	**45.13**
		Specimen no. 2	1.53	51.6	3.1	
	2wt%	**Specimen no. 1**	1.32	44.5	3.6	**53.93**
		Specimen no. 2	1.33	46.3	3.4	
	3wt%	**Specimen no. 1**	1.43	50.0	2.3	**57.72**
		Specimen no. 2	1.36	39.5	2.5	
	4wt%	**Specimen no. 1**	1.40	33.0	2.7	**57.405**
		Specimen no. 2	1.34	34.3	2.9	

Table 5.7 Results of specimens from NaOH Bath at 45^0C

NaOH at 45^0C						
No. of Days	**Specimen Name**	**Specimen No.**	**Elastic Modulus (GPa)**	**Flexural Strength (MPa)**	**Deformation At Max. Force %**	**% Decrease in Strength**
0 Day	**0wt%**	**Specimen no. 1**	0.715	81.7	1.5	
		Specimen no. 2	0.662	72.71	1.7	
	0.5wt%	**Specimen no. 1**	5.96	105	1.6	
		Specimen no. 2	3.95	66.5	1.6	
	2wt%	**Specimen no. 1**	4.43	102	1.9	
		Specimen no. 2	3.50	95.1	1.6	
	3wt%	**Specimen no. 1**	7.02	114	1.6	
		Specimen no. 2	6.52	97.7	1.2	
	4wt%	**Specimen no. 1**	3.90	72.6	2.8	
		Specimen no. 2	4.63	85.4	2.1	
30 Days	**0wt%**	**Specimen no. 1**	1.72	12.7	1.0	**80.57**
		Specimen no. 2	0.692	17.3	2.9	
	0.5wt%	**Specimen no. 1**	1.38	19.0	0.99	**77.32**
		Specimen no. 2	1.46	19.9	1.0	
	2wt%	**Specimen no. 1**	1.56	27.7	1.3	**75.49**
		Specimen no. 2	1.58	20.6	0.93	
	3wt%	**Specimen no. 1**	1.40	19.1	0.98	**79.49**
		Specimen no. 2	1.78	24.3	0.95	
	4wt%	**Specimen no. 1**	0.852	14.5	1.1	**75.19**
		Specimen no. 2	1.50	24.7	1.1	

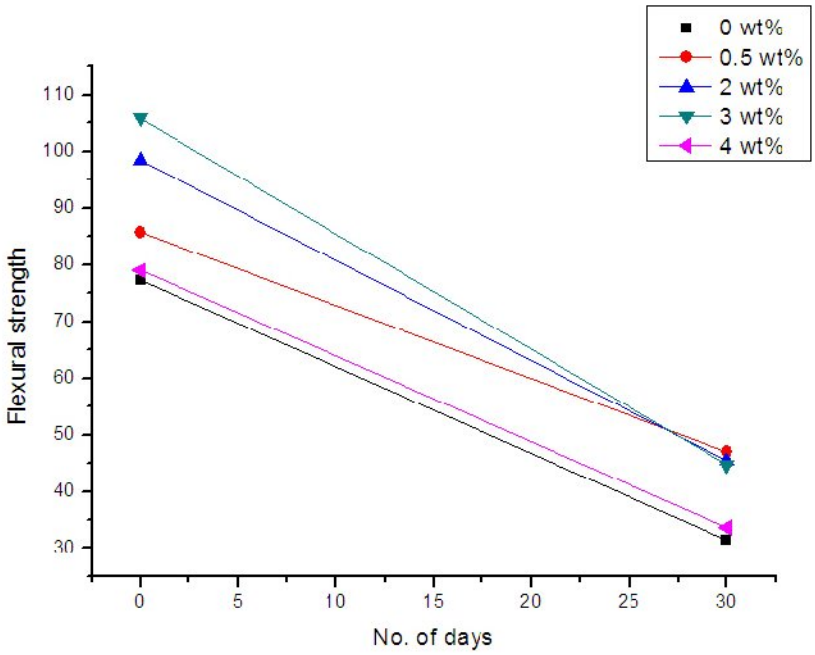

Fig. 5.13 Flexural strength degradation (Water bath at 45^0C)

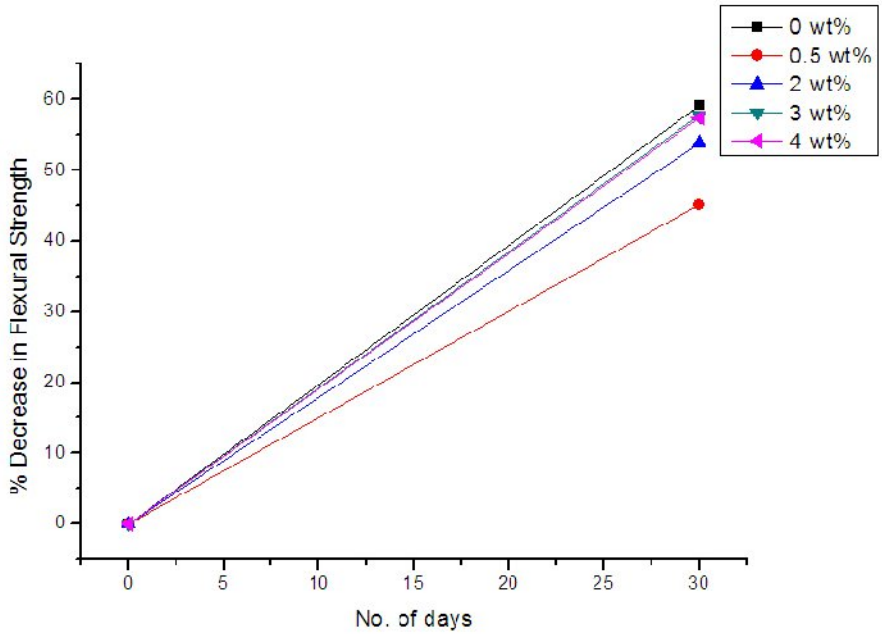

Fig. 5.14 Percent decrease in flexural strength (Water bath at 45^0C)

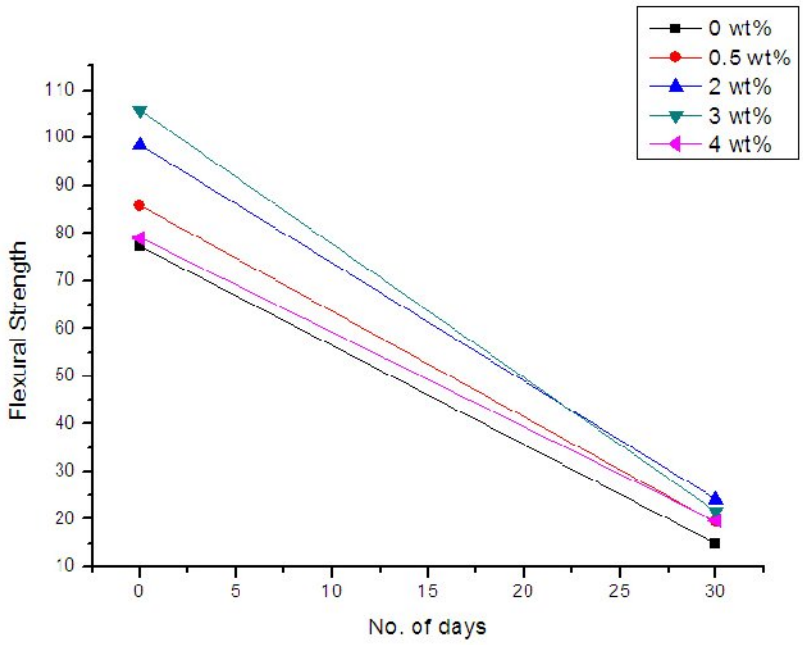

Fig. 5.15 Flexural strength degradation (NaOH bath at 45^0C)

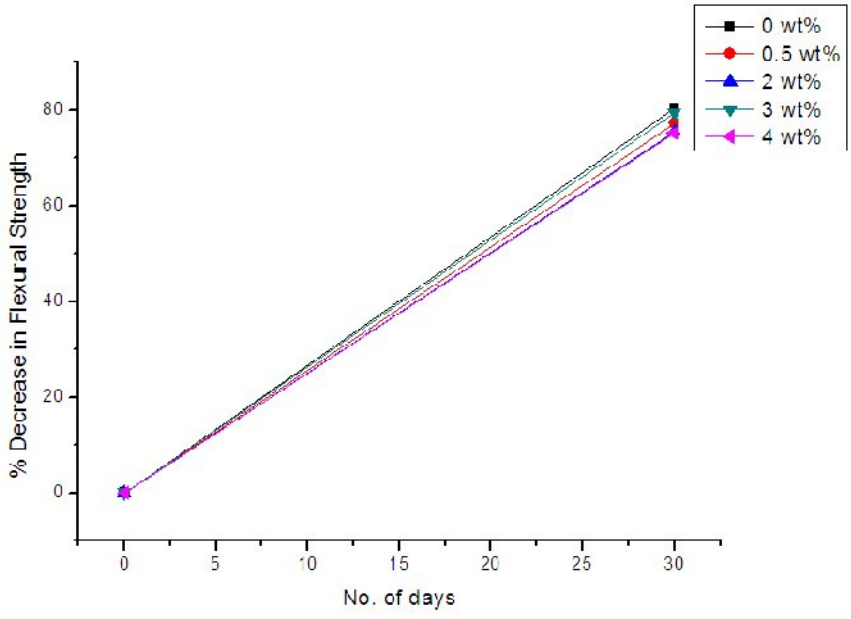

Fig. 5.16 Percent decrease in flexural strength (NaOH bath at 45^0C)

From tables 5.4 and 5.5, the water immersion of 3 wt% specimen results in 57.72% decrease in flexural strength but the NaOH immersion of 3 wt% specimen results in 79.49% decrease in flexural strength which showed that there is tremendous decrease in flexural strength of specimens immersed in NaOH as compared to specimens immersed in water.

CHAPTER 6 CONCLUSION AND FUTURE SCOPE

6.1 Conclusion

Two different areas of characterization instruments were employed to study the mechanical and microstructural behaviors of the nanoclay-epoxy samples. From the mechanical instruments such as Zwick/Roell universal testing machine and Vickers' hardness tester, the ultimate tensile strength, flexural strength and Vickers' hardness values were obtained. From the microstructural analysis instruments such as X-Ray Diffractometry (XRD), the positions of the diffraction peaks of the samples were obtained.

From the Vickers' hardness results of the nanoclay-epoxy specimens, the 2wt% nanoclay sample was the hardest among all the compositions with the largest HV value of 7.535 when compared with that of pure epoxy sample of HV 4.308, an increase of 43% in Vickers' hardness value. And 3wt% nanoclay sample showed a drop in the hardness with value of HV 5.282. This might be attributed to the possible aggregation of nanofillerclay at some sites. From the XRD results, the absence of peaks in diffraction pattern indicates formation of exfoliated nanocomposites at all levels of nanoclay loading.

From the tensile results, 3wt% nanoclay loading specimen showed the highest value of tensile strength which is 27% higher than neat epoxy glass fiber reinforced composite. The increase in the strength of the epoxy samples must be due to the introduction of nanoclay, which shares the stress imposed on the polymer chain. The individual platelets have much higher mechanical properties as compared to polymer matrix. However, the reason for the sudden drop in the ultimate tensile strength in 2wt% nanoclay was not clear. From the flexural results, when compared with neat epoxy-glass composites, 37% improvement in strength of specimen with 3wt% clay loading was observed. With further increase in nanoclay loading, the strength reduced significantly. Tensile strength and flexural strength of the 3 wt% clay content sample was improved.

The durability studies were conducted on nanocomposites by exposing to water and alkaline medium for a period of one month then evaluating the mechanical property degradations. Mechanical properties were found to degrade with increase in due time. The properties

degradation in NaOH environment was more severe as compared to simple water. The water resistance property of epoxy was improved by the addition of both glass fibre and nanoclay, which is might be attributed to the increasing of the tortuosity path for water penetration.

6.2 Future scope

1. To see the effect of nanofillers on FRP`s, experiments can be repeated by changing the type of nanofillers.
2. The experiment can be done by placing fiber sheets at different orientations.
3. The experiments can be performed on polyester as matrix system, since with this matrix the barrier properties of composites can be enhanced.
4. Clay loading can also be varied more than 5 wt%.
5. The duration of current experiment can be increased to see the effect in long term.
6. The strength of alkaline aqueous solution can be varied to see the change in chemical attack.

REFERENCES

1. **Alexandre M,** (2000), Polymer-layered Silicate Nanocomposites: Preparation, Properties and uses of a New Class of Materials, Mater. Sci. Eng. Rep., 28, 1-63.
2. **Avila A, Almir S and Marcelo I.,** (2006), A study on nanostructured plates behaviour under low-velocity impact loading. Material and design, 34, 28-41.
3. **Avila A, Horacio V. and Marcelo I.,** (2005), The nanoclay influence on impact response of laminated plates, Latin American journal of solids and structures, 3, 3-20.
4. **Berketis K, Tzetzis D and Hogg P.J,** (2007), The influence of long term water immersion ageing on impact damage behaviour and residual compression strength of glass fiber reinforced polymer (GFRP), Material and design, 29, 1300-1310.
5. **Biron, M.,** (1973), Thermosets and Composites-Technical Information for Plastics Users, New York: Elsevier.
6. **Chow W, Bakar A and Ishak Mohamad A.,** (2005), Water absorption and hygrothermal aging study on organomontomorrillonite reinforced polyamide6/polypropylene nanocomposites, Journal of applied polymer science, vol 98, 780-790.
7. **Gao Shang-Lin, Mader E and Plonka R.,** (2007), Nanocomposite coating for healing surface defects of glass fiber and improving interfacial adhesion, Composite science and technology, 68, 2892-2901.
8. **Han S. O., Dzarl L. T.**, (2003), Water absorption effects in hydrophilic polymer matrix of carboxyl functionalized glucose resin and epoxy resin. European Polymer Journal, 39, 1791–1799.
9. **Hossain M. K., Imran K. A., Hosur M. V. and Jeelani S.,** (2011), Degradation of Mechanical properties of convectional and nanophased Carbon/Epoxy composites in seawater.
10. **Jena P,** (1996), Nanostructured materials**,** Nova Science New York.
11. **Karad S. K., Attwood D.**, (2005), Jones F. R.: Moisture absorption by cyanate ester modified epoxy resin matrices, Part V: Effect of resin structure, Composites: Part A, 36, 764–771.

12. **Kornmann X, Rees M, Thomsan Y, Necola A, Barbezat M and Thomsan R,** (2005), Epoxy layered silicate nanocomposite as matrix in glass fiber-reinforced composites, Composite science and technology, 65, 2259-2268.
13. **Lei Wang, Ke Wang, Ling Chen and Chaobin He,** (2006), Hydrothermal Effects on the Thermo-mechanical Properties of High Performance Epoxy/Clay Nanocomposites, Polymer engineering science, 46, 215–221.
14. **Lin Li-Yu, Lee Joong-Hee, Hong Chang-Eui, Yoo Gye-Hyoung, Advani Suresh G,** (2005), Preparation and characterization of layered silicate/glass fiber/epoxy hybrid nanocomposites via vacuum-assisted resin transfer moulding (VARTM), Composites Science and Technology 66 (2006) 2116–2125.
15. **Lowenstein, K. L.** (1973), Manufacturing Technology of Continuous Glass Fibers, New York: Elsevier.
16. **Manjunatha C.M, Taylor A.C, Kinloch A.J and Sprenger S,** (2009), The tensile fatigue behavior of a silica nanoparticle-modified glass fiber reinforced epoxy composites, Composite science and technology, 70, 193-199.
17. **Njuguna J and Pielichowski K,** (2003), Advanced Engineering Materials, 5, 769.
18. **Ohsawa T, Miwa M, Kawade M**, (1990), Axial compressive strength of carbon fiber. J App Polym Sci 39, 1733-1743
19. **Quaresimin M. and Varley R. J,** (2007),Understanding the effect of nano-modifier addition upon the properties of fiber reinforced laminates, Composite science and technology, 68, 718-726.
20. **Qutubuddin S., Fu X.**, (2001), Nano-Surface Chemistry, (New York, NY, USA), pp. 653-672.
21. **Rumiana K,** (1994), Thermoset Nanocomposites for Engineering Applications.
22. **Sakaki H and Noge H., eds,** (1994), Springer Verlag, Berlin.
23. **Sinha R. S., Okamoto M.,** (2003), Polymer/layered silicate nanocomposites: a review from preparation to processing, Prog. Polym. Sci., 28, 1539–1641.
24. **Wang H, Zeng C, Elkovitch M and Koelling W. K,** (2001), Processing and properties of polymeric nanocomposites, Polymer engineering and science, 41, 11.
25. **Wetzel B, Haupert F, Zhang MQ,** (2003) Epoxy nanocomposites with high mechanical and tribological performance. Compos Sci Technol , 63, 2055-2067

26. **Wetzel B, Rosso P, Haupert F and Friedrich K,** (2006), Epoxy nanocomposite-fracture and toughening mechanisms, Engineering fracture mechanics, 73, 2375-2398.
27. **Yasmin A, Luo J.J, Abot J.L, Danial I.M,** (2006), Mechanical and thermal behavior of clay/epoxy nanocomposites, Composite science and technology, 66, 2415-2422.
28. **Zafar A, Bertocco F, Schjodt-Thomsen J and Rauhe J.C**, (2012), Investigation of the long term effects of moisture on carbon fibre and epoxy matrix composites, Composite science and technology.
29. **Zainuddin S, Hosur M.V, Zhou Y, Kumar Ashok and Jeelani S,** (2010), Durability study of neat/nanophased GFRP composite subjected to different environmental conditioning, Material science and engineering, A 57, 3091-3099.
30. **Zhou J., Lucas J. P.**, (1999), Hygrothermal effects of epoxy resin. Part 1: The nature of water in epoxy. Polymer, 40, 5505–5512.
31. http://etd.ohiolink.edu/view.cgi?acc_num=akron1216947385.
32. http://library.iyte.edu.tr/tezler/master/malzemebilimivemuh/T000538.pdf.